The dynamical holographic QCD method for QCD matter

Yidian Chen
陈亦点

School of Physics, Hangzhou Normal University

Based on arXiv: 2405.06386, 2408.17080

Oct. 26, 2024

Outline

I. Introduction

II. QCD phase transition under rotation

III. Pion Condensation

IV. Conclusion and discussion

I. Introduction

Gauge/Gravity duality

AdS/CFT correspondence

J. M. Maldacena, Adv. Theor. Math. Phys. **2**, 231 (1998)

relates gravity theories on anti-de Sitter spacetimes (AdS) to conformal field theories

General Gauge/Gravity duality

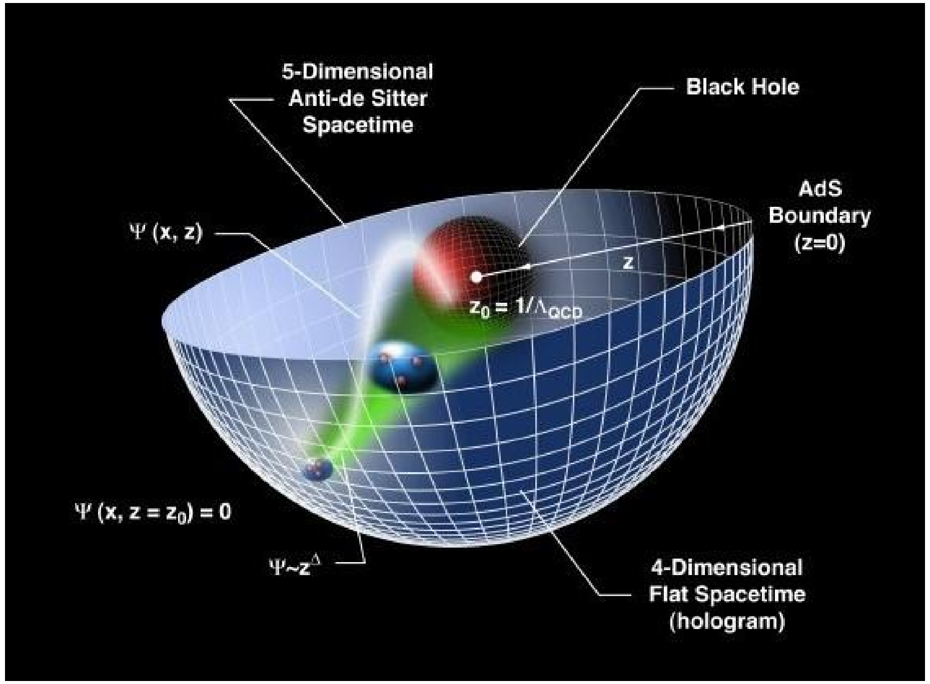

The Renormalization Group Flow

Adams, Allan et al.
New J.Phys.(2012),
arXiv:1205.5180

$$H = \sum_{x,i} J_i(x)\mathcal{O}^i(x)$$

J(x): coupling constant or source for the operator

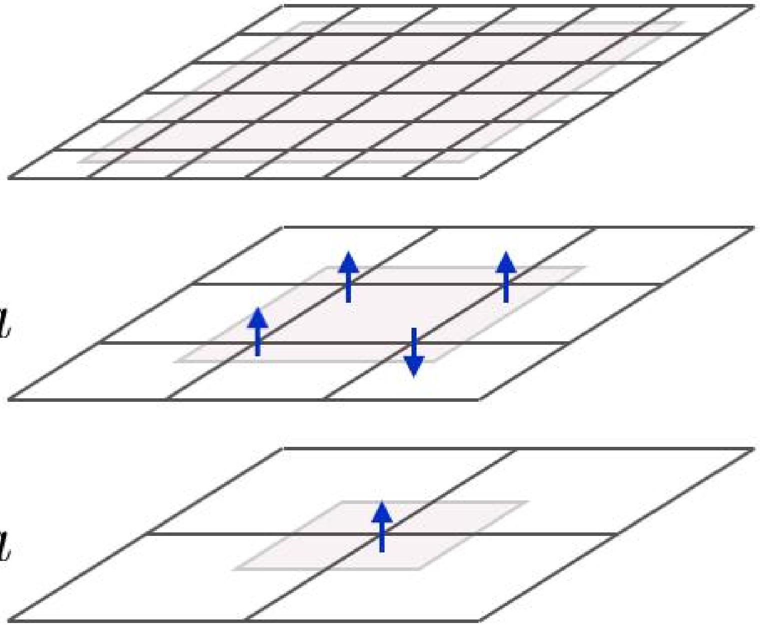

a $$H = \sum_i J_i(x, a)\, \mathcal{O}^i(x)$$

$2a$ $$H = \sum_i J_i(x, 2a)\, \mathcal{O}^i(x)$$

$4a$ $$H = \sum_i J_i(x, 4a)\, \mathcal{O}^i(x)$$

$$u\frac{\partial}{\partial u} J_i(x, u) = \beta_i(J_j(x, u), u)$$

Holographic Duality & RG flow

Adams, Allan et al.
New J.Phys.(2012),
arXiv:1205.5180

QFT on lattice
RG scale
Coupling constant

Gravitational problem
Extra spatial dimension
Dynamical field

$$J_i|_{UV} = \Phi_i|_{\partial}$$

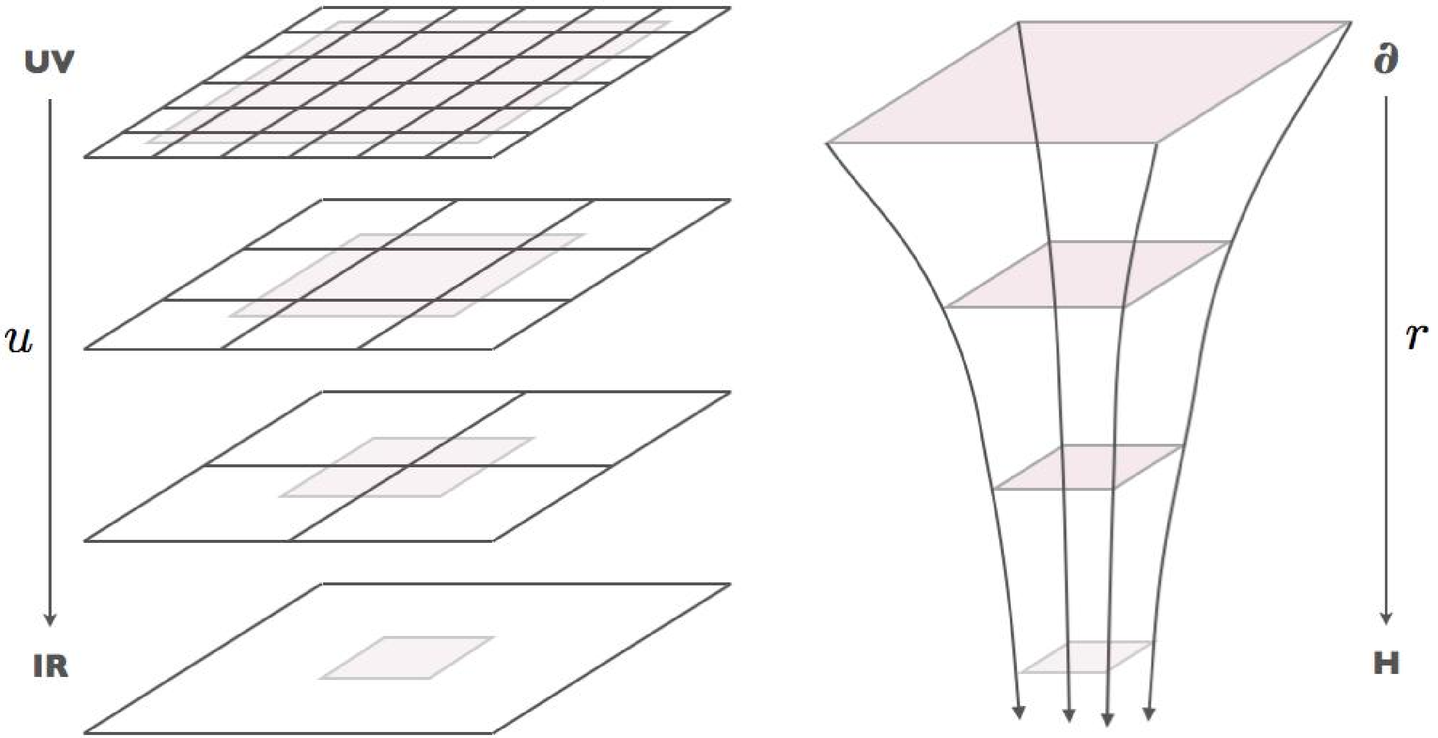

QCD

Effective field theories and models

QM, NJL, SM, HLS,

CHPT, NRQCD,

color flux tube,

Dual superconductor ……

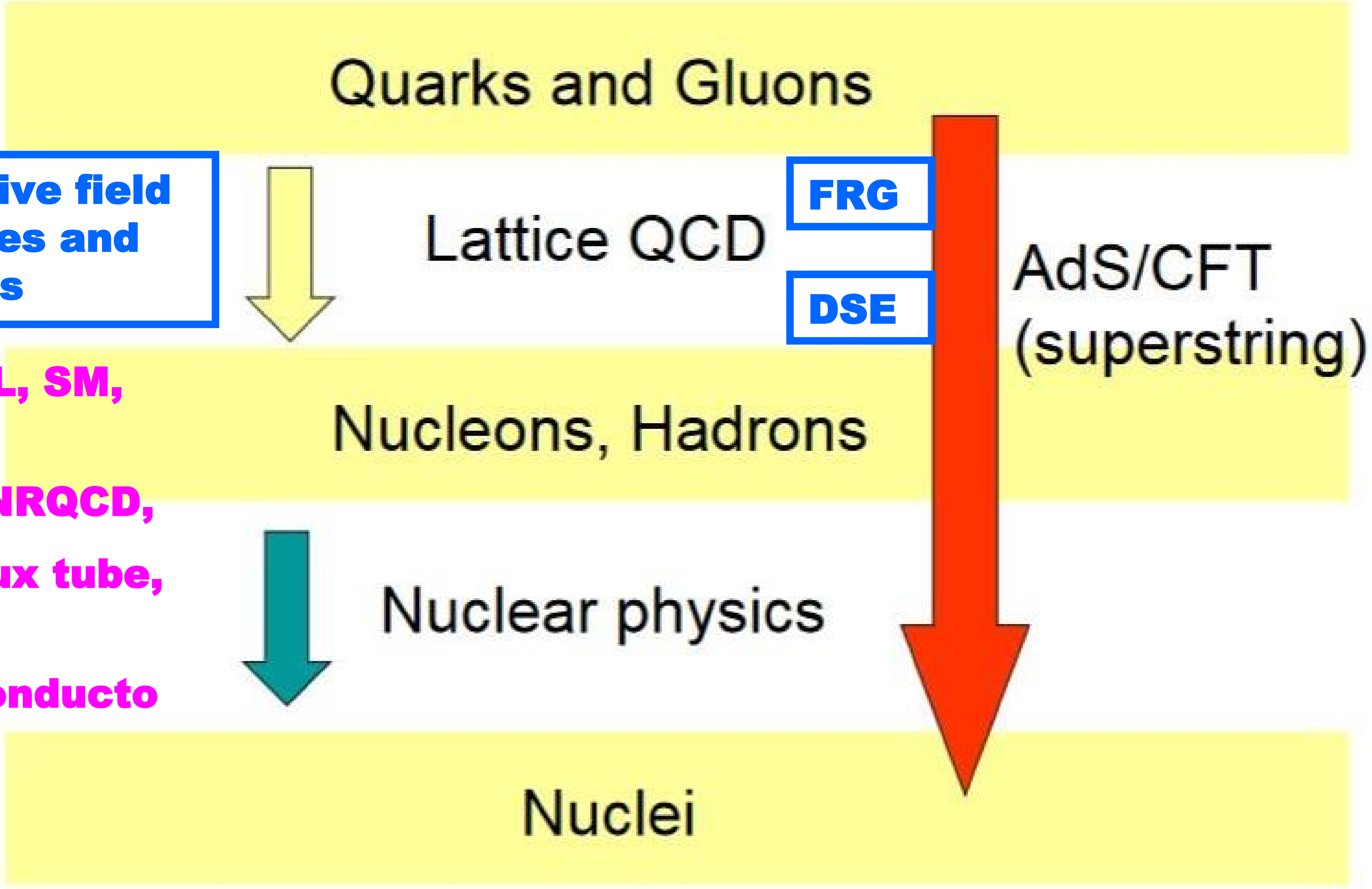

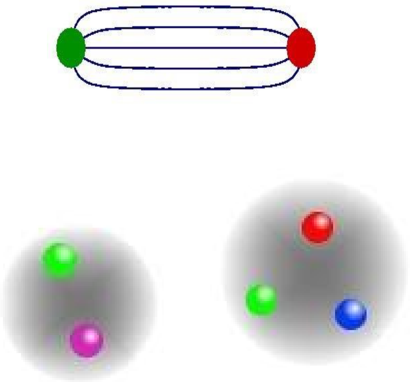

Top-down vs Bottom-up

Top-down：based on string theory and D-brane

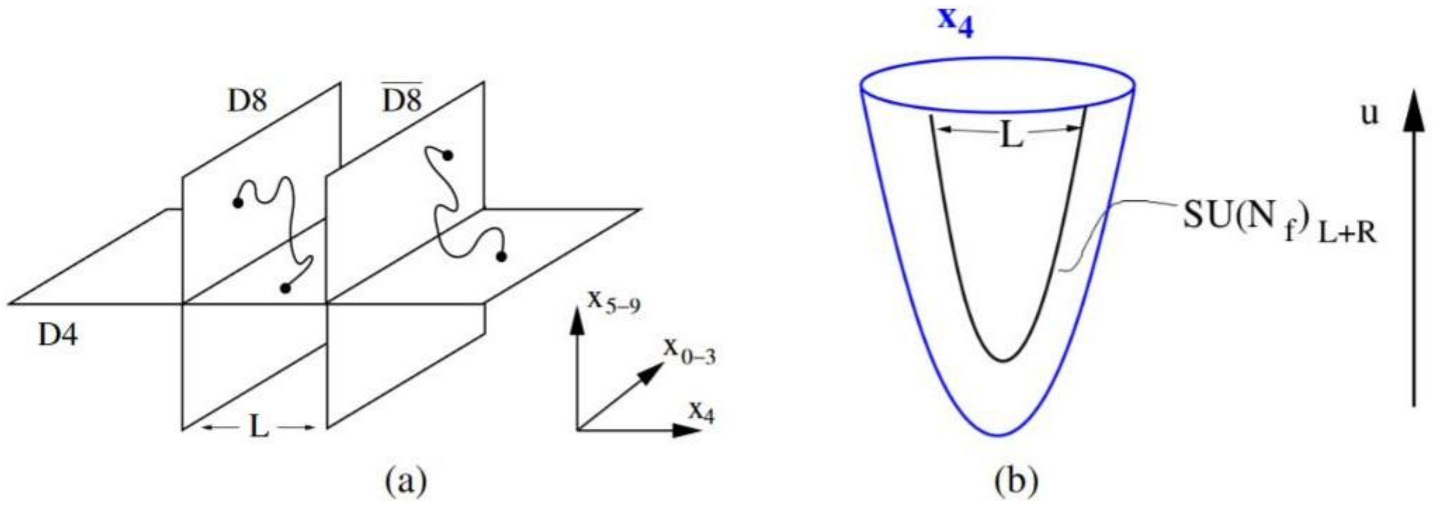

D3-D7,
D4-D6,
D4-D8,
STU model
…

Bottom-up：from symmetry of QCD

hard-wall, soft-wall, Gubser model, improved holographic QCD, dynamical holographic QCD …

1) **5D effective action**
2) **IR cutoff or dilaton to realize confinement**

Hadron spectra, chiral symmetry breaking & linear confinement, phase transitions, equation of state, transport properties

Holographic dictionary

Boundary QFT | **Gravity**

Local operator $\mathcal{O}_i(x)$ | **Field** $\Phi_i(x,r)$

conformal dimension Δ, p-form field p $\quad (\Delta - p)(\Delta + p - d) = m_5^2 L^2$

Strongly coupled | **Weakly coupled semi-classical**

$$\boxed{Z_{\mathrm{QFT}}[J_i] \;=\; Z_{\mathrm{QG}}[\Phi[J_i]]}$$

$$Z_{\mathrm{QFT}}[J] \;\simeq\; e^{-I_{\mathrm{GR}}[\Phi[J]]}$$

$$\langle \mathcal{O}_1(x_1)\ldots\mathcal{O}_n(x_n)\rangle = \frac{\delta^n I_{\mathrm{GR}}[\Phi[J_i]]}{\delta J_1(x_1)\ldots\delta J_n(x_n)}\bigg|_{J_i=0}$$

5D action of DHQCD

Chen et al., Commun. Theor. Phys., arXiv: 2206.00917

5D action

$$S_{DHQCD} = S_{GDM} + \lambda S_{KKSS}$$

Dilaton profile

$$\Phi(z) = \mu_G^2 z^2$$

the Graviton–Dilaton–Maxwell action in the string frame

$$S_{GDM} = \frac{1}{16\pi G_5}\int d^5x\sqrt{-g}e^{-2\Phi}\left[R + 4(\partial\Phi)^2 - V(\Phi) - \frac{h(\Phi)}{4}F^2\right]$$

The action of KKSS model takes the following form

$$S_{KKSS} = -\int d^5x\sqrt{-g}e^{-\Phi}Tr\left[|DX|^2 + V_X + \frac{1}{4}\left(F_L^2 + F_R^2\right)\right]$$

DHQCD for Hadron Physics

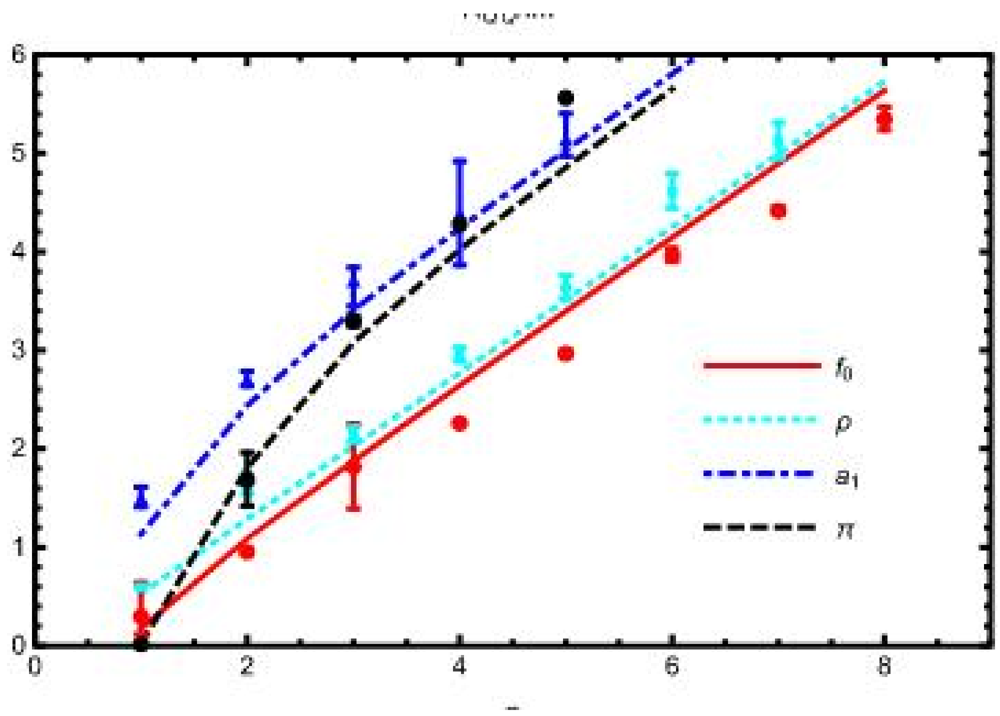

Li et al., JHEP(2013)

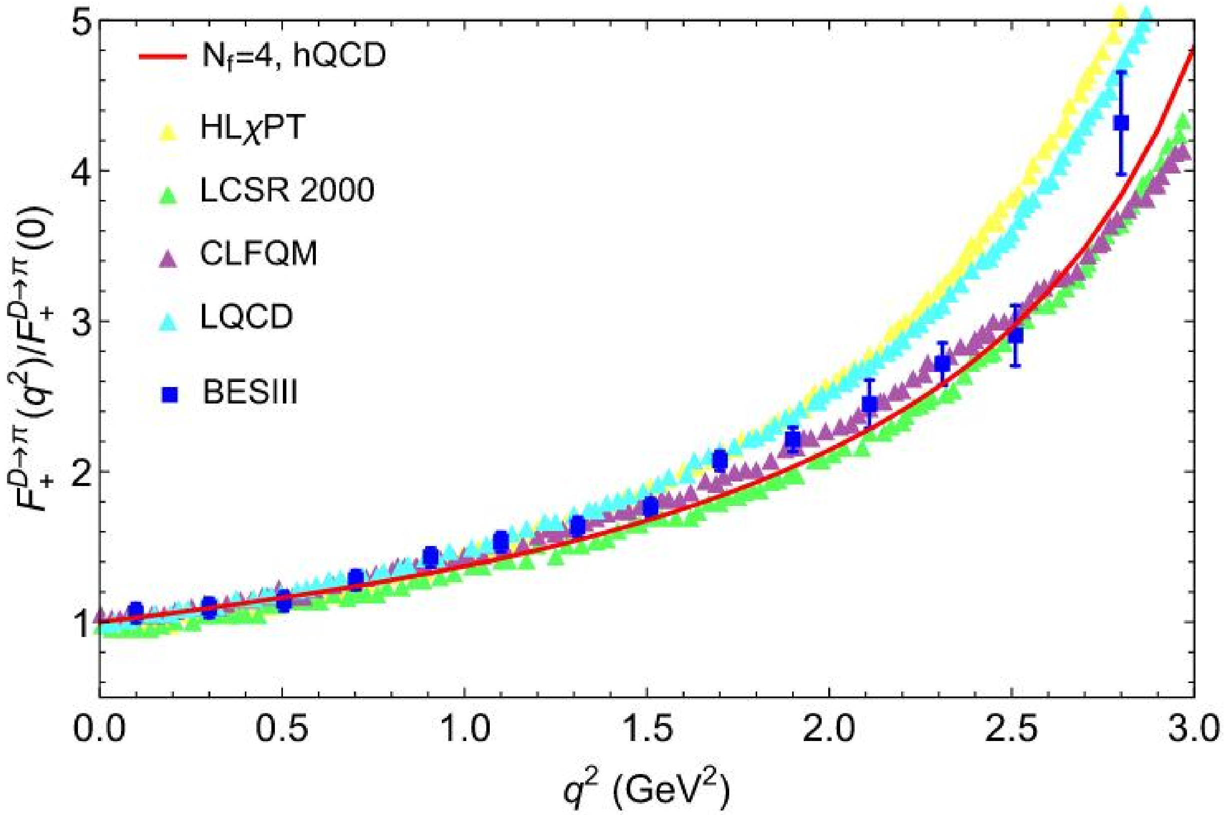

Chen et al., PRD(2022)
Ahmed et al., PRD108.086034 (2023)
Ahmed et al., PRD109.026008 (2023)

Results of the light meson spectra and semileptonic form factor from the DHQCD model

DHQCD for QCD Phase Transition

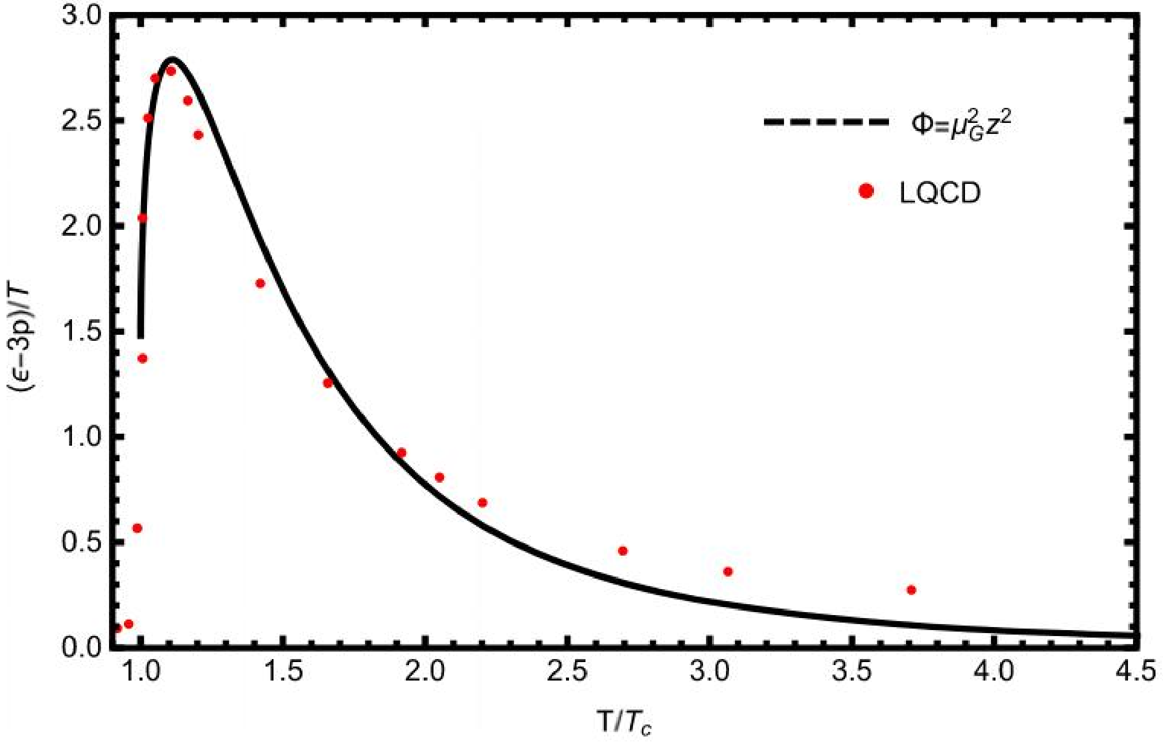

Li et al., JHEP(2011)

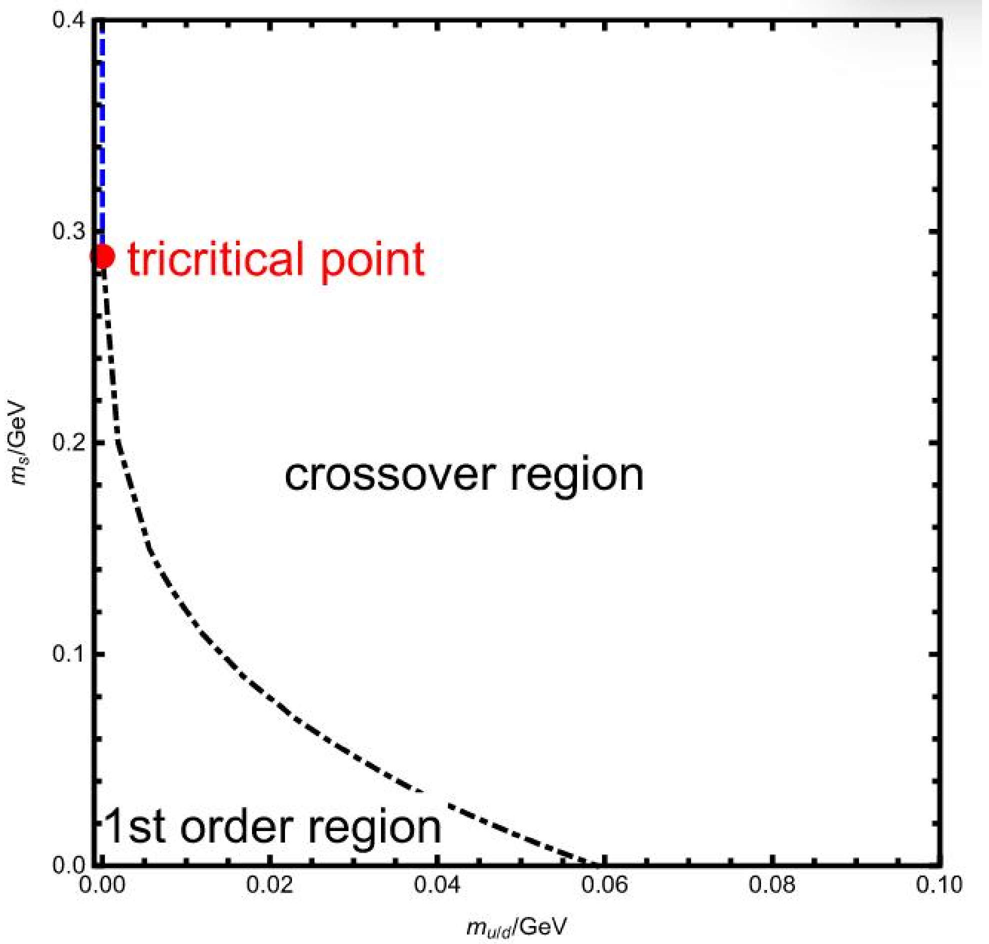

Chelabi et al., PRD(2016)
Chelabi et al., JHEP(2016)

DHQCD for QCD Phase Transition

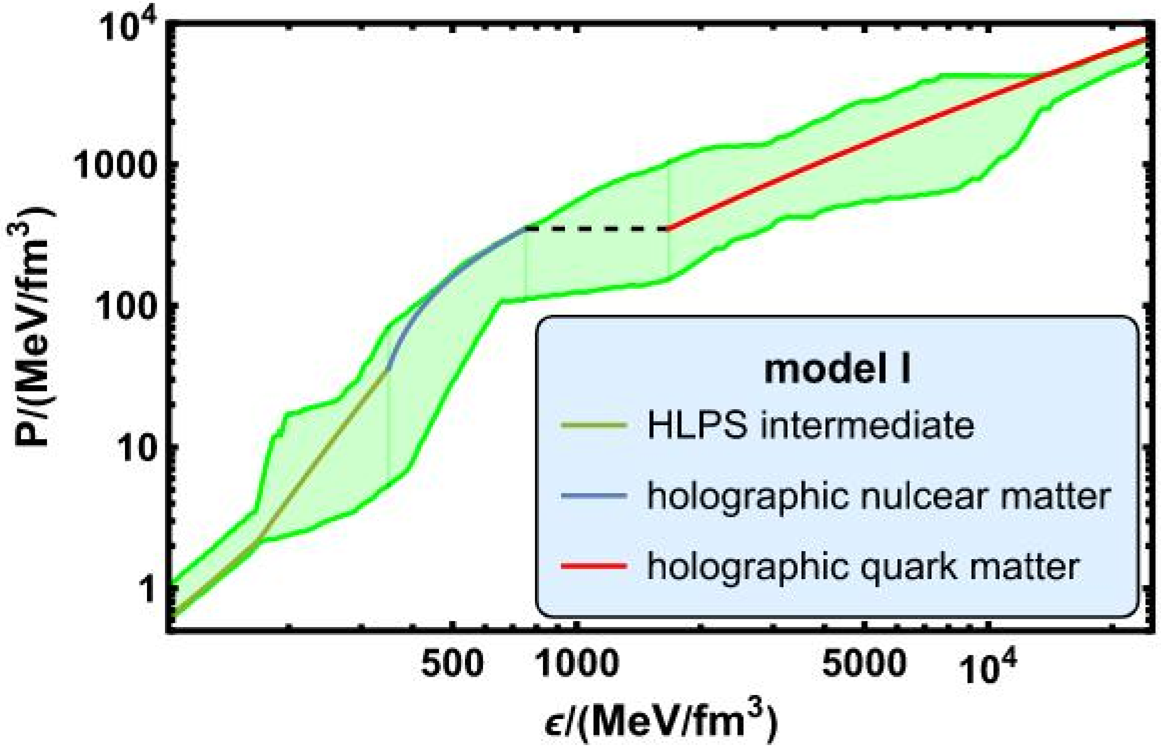

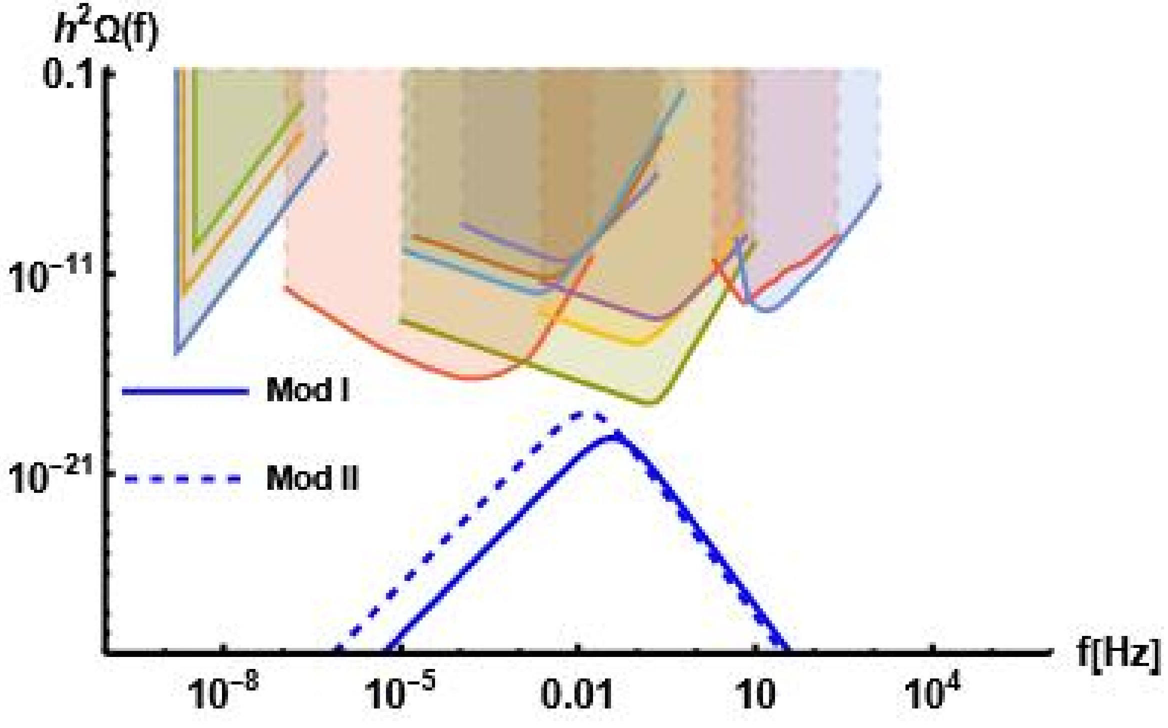

(a)

Zhang et al., PRD(2022)

Chen et al., JHEP(2018)
Chen et al., JHEP(2023)

II. QCD phase transition under rotation

Heavy Ion Collision

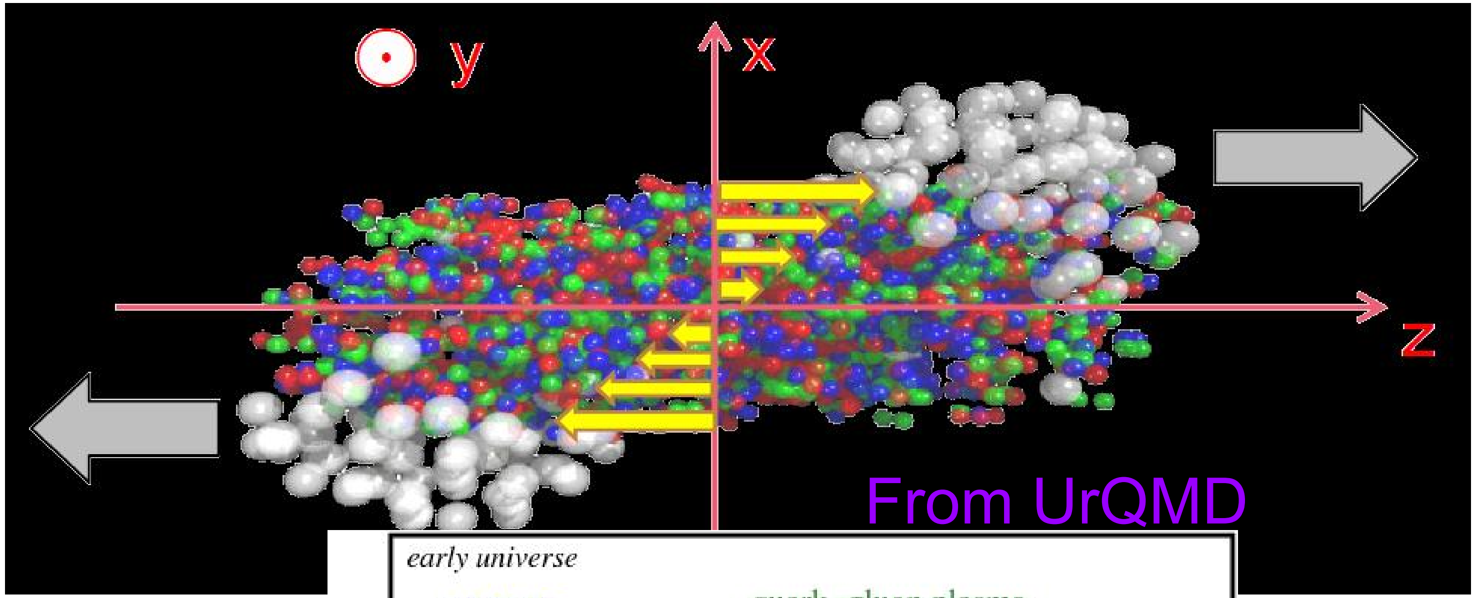

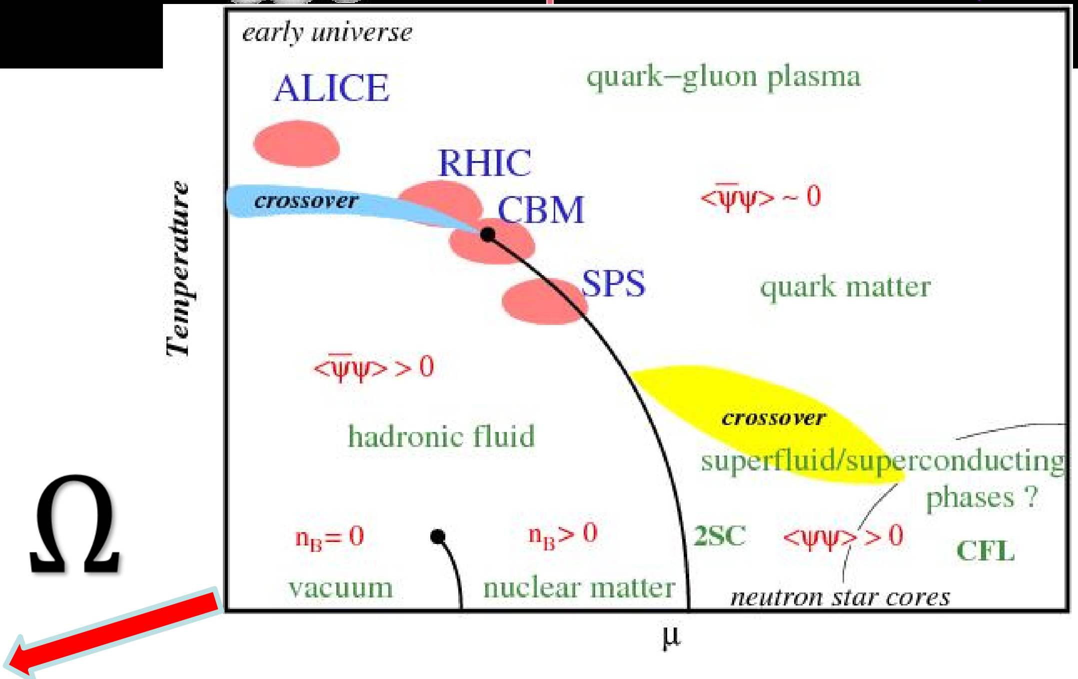

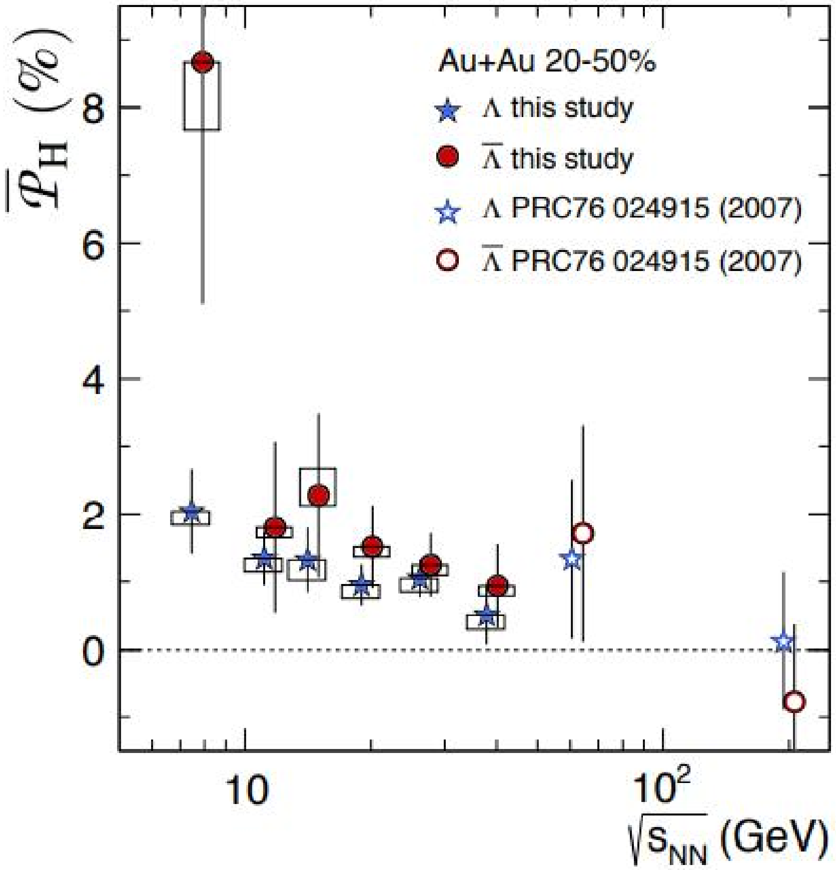

L. Adamczyk, et al. (STAR), Nature 548 (2017) 62.

Models

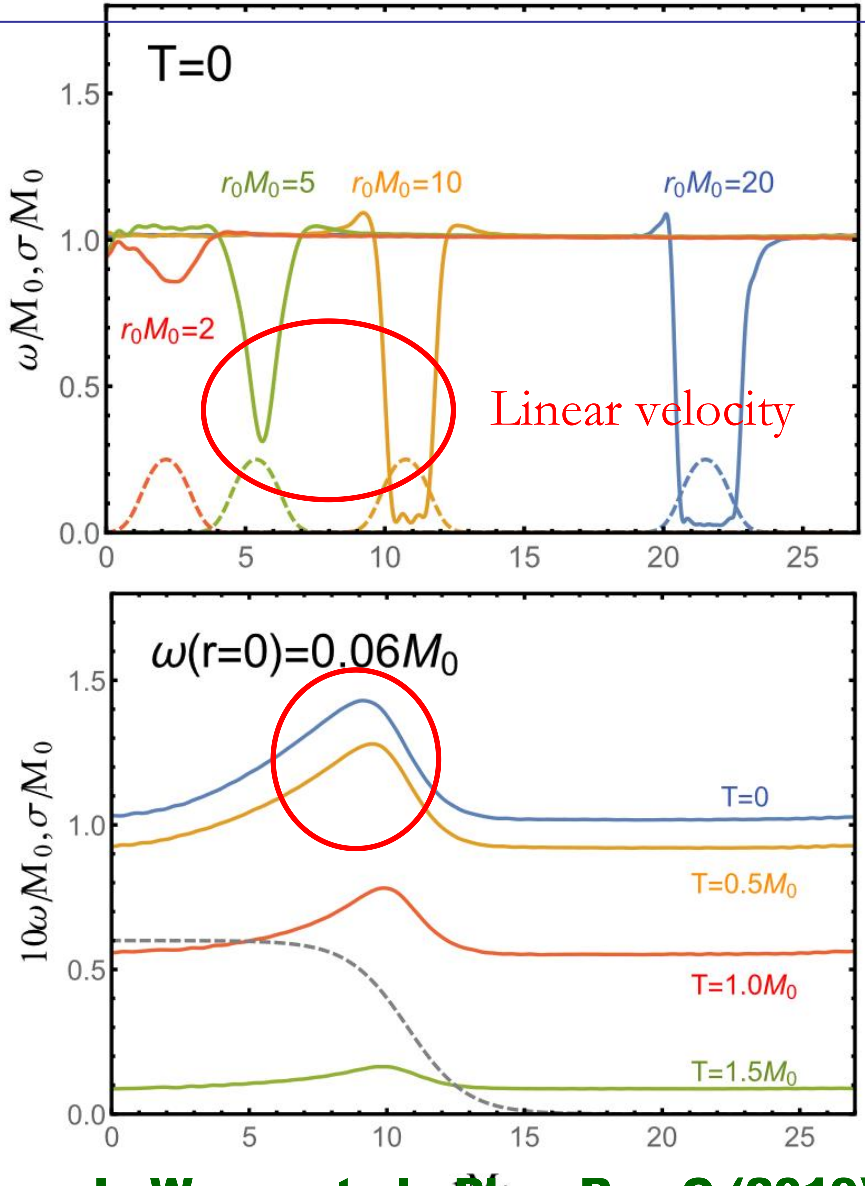

L. Wang, et al., Phys.Rev.C (2019)

Suppression

Centrifugal-like effect

$T-\Omega$ phase diagram

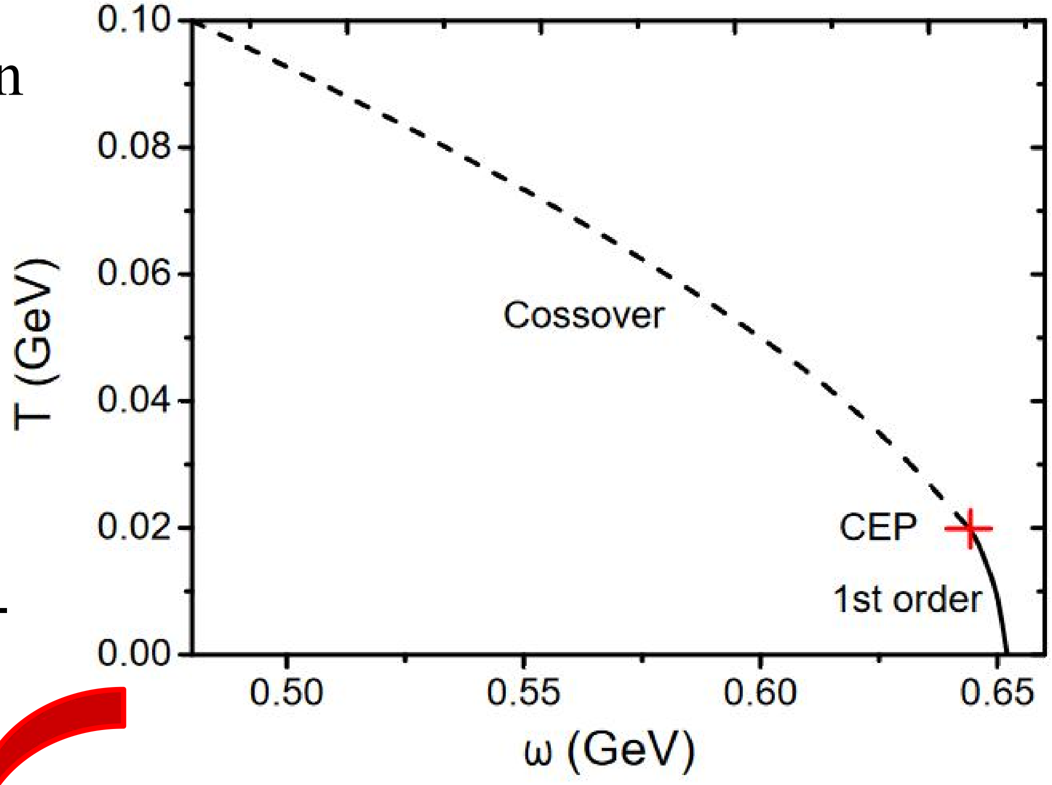

Y. Jiang, et al., Phys.Rev.Lett (2016)

Similar to chemical potential μ

Lattice QCD

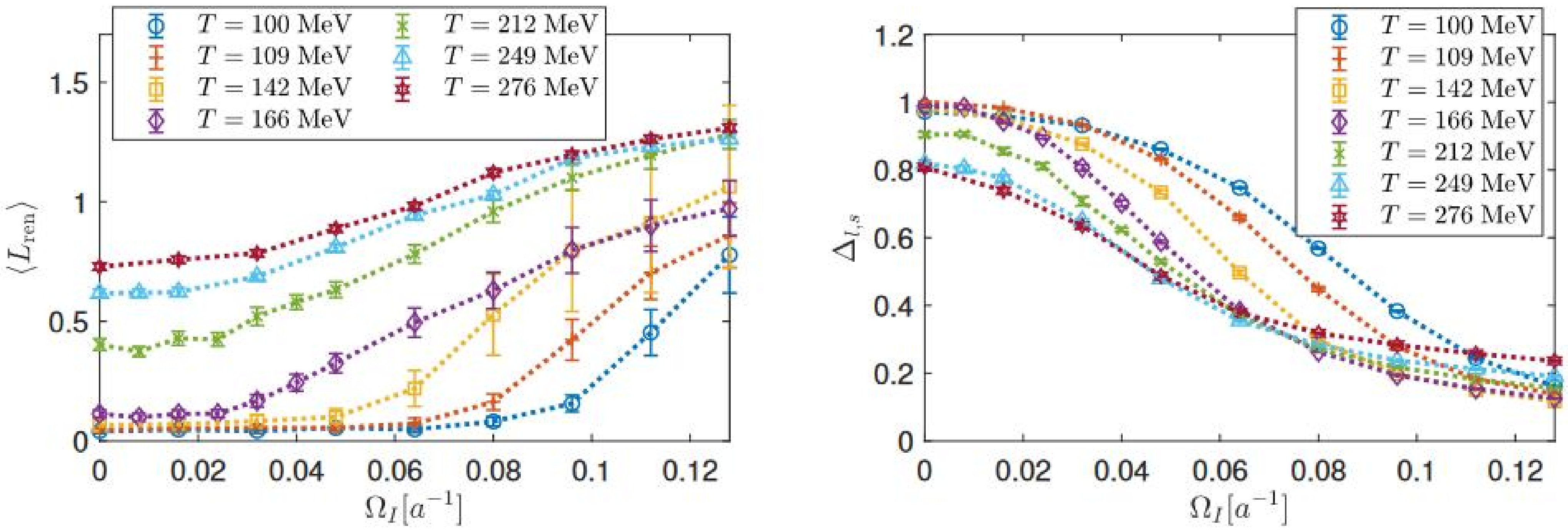

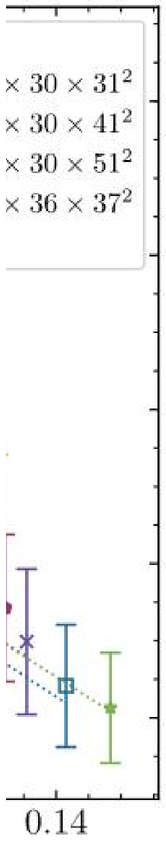

J. Yang, X. Huang, arXiv: 2307.05755

FIG. 4. The Polyakov loop and chiral condensate as functions of Ω_I.

analytically continued to real
angular velocity.

V.V. Braguta, et al., Phys.Rev.D (2021)

Holographic results

Deconfinement phase transition

1). Kerr-AdS black hole

2). Doing a local Lorentz boost

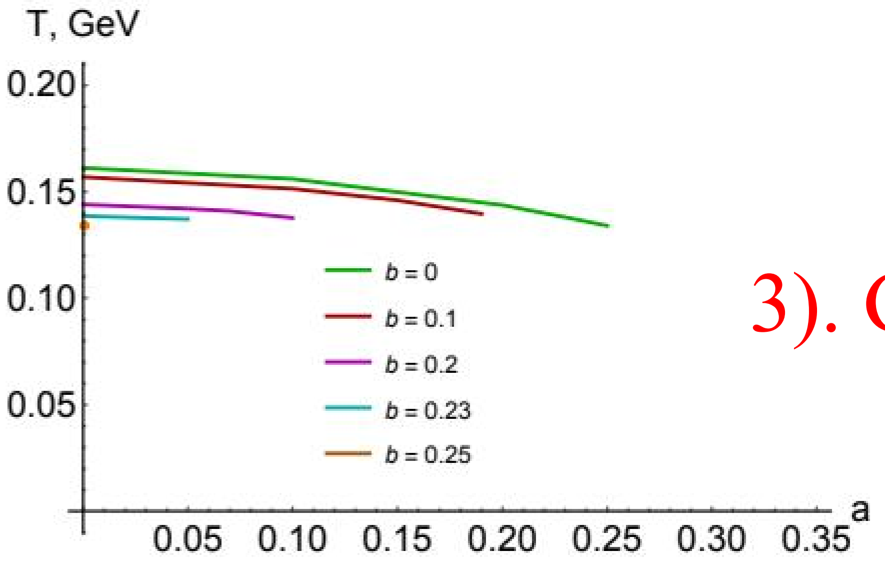

A

3). Gauge Field

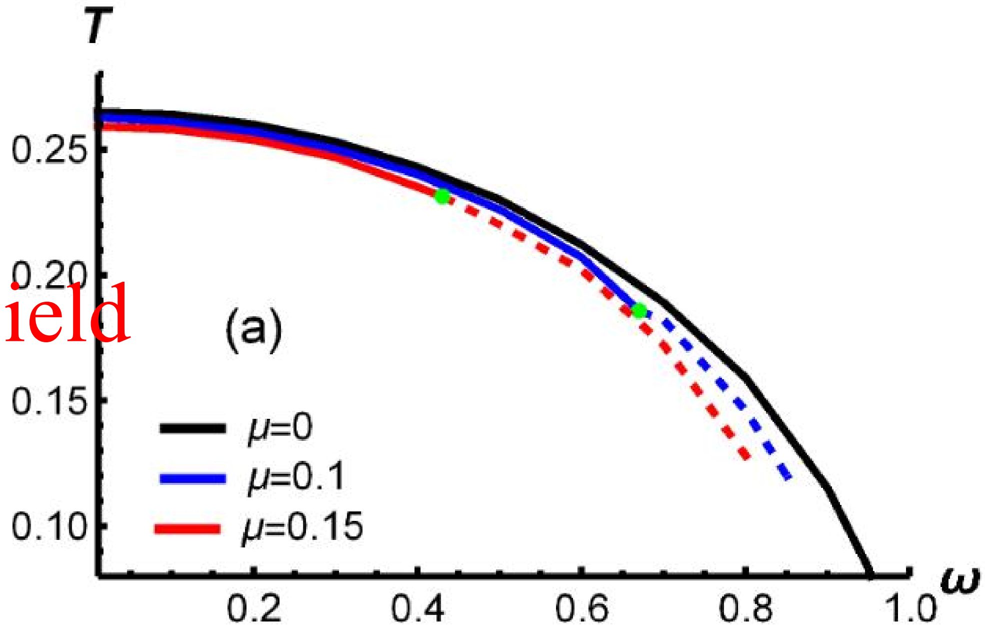

I.Y. Aref'eva, et al., JHEP (2021)

X. Chen, et al., JHEP (2021)

Chiral Condensation

Chelabi et al., Phys.Rev.D (2016)
Chelabi et al., JHEP (2016)

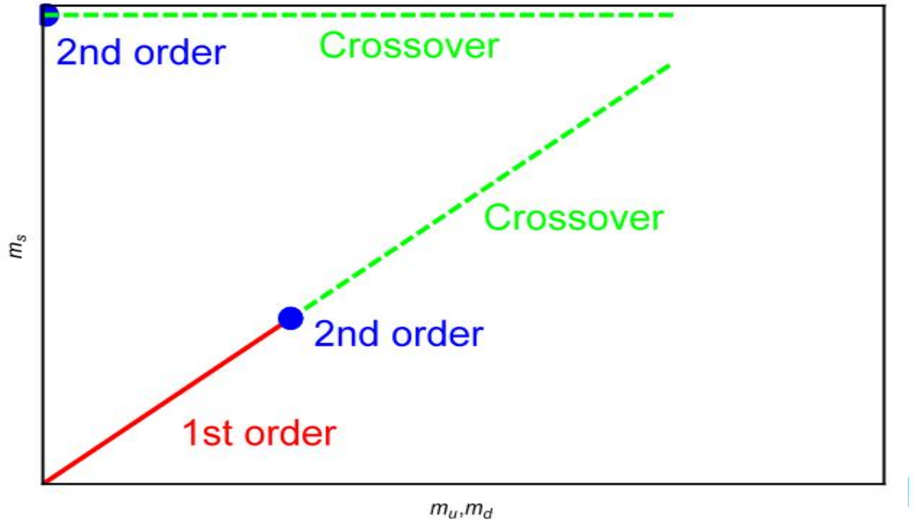

(a)

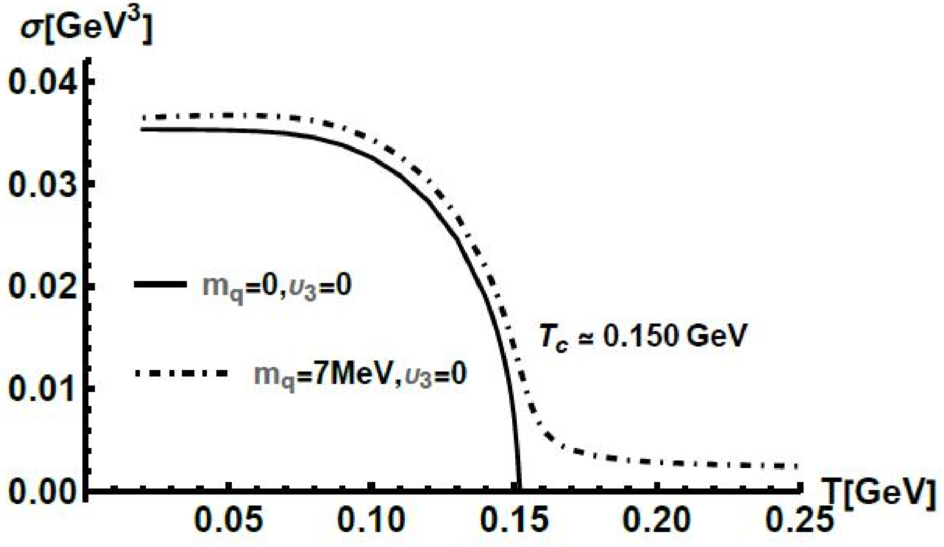

(b)

5D action

$$S = -\int d^5x\sqrt{-g}e^{-\Phi}Tr(D_mX^+D^mX + V_X(|X|)).$$

$$V(\chi) \equiv Tr(V_X(|X|)) = -\frac{3}{2}\chi^2 + v_3\chi^3 + v_4\chi^4.$$

$$\Phi(z) = -\mu_1 z^2 + (\mu_1 + \mu_0)z^2 \tanh(\mu_2 z^2),$$

TABLE I: Operators/fields of the model

4D: $\mathcal{O}(x)$	5D: $\phi(x,z)$	p	Δ	$(m_5)^2$
$\bar{q}_L\gamma^\mu t^a q_L$	$A^a_{L\mu}$	1	3	0
$\bar{q}_R\gamma^\mu t^a q_R$	$A^a_{R\mu}$	1	3	0
$\bar{q}^\alpha_R q^\beta_L$	$(2/z)X^{\alpha\beta}$	0	3	-3

Conformal AdS$_5$

$$ds^2 = \frac{L^2}{z^2}(dz^2 + \eta_{\mu\nu}dx^\mu dx^\nu),$$

Model

Y. Chen, Danning Li and M. Huang, Phys.Rev.D (2022)

Metric $$ds^2 = \frac{L^2}{z^2}[-f(z)dt^2 + \frac{dz^2}{f(z)} + dr^2 + r^2 d\theta^2 + dx_3^2],$$ $$f(z) = 1 - (\frac{z}{z_h})^4$$

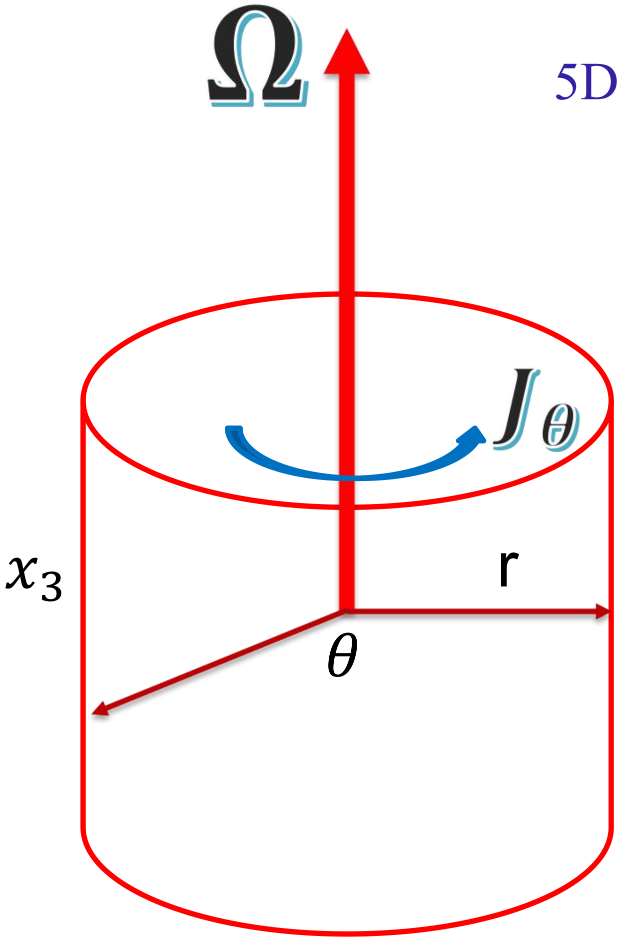

5D action $$S_M = -\int d^5x\sqrt{-g}e^{-\Phi(z)}\left\{\mathrm{Tr}[(D^M X)^\dagger(D_M X) + V_X(|X|)] + \frac{1}{4}F_{MN}F^{MN}\right\},$$

The only nonzero component of the gauge field is A_θ, which is dual to the polar current operator $\langle\bar{q}\gamma_\theta q\rangle$ and described an effective polarization term $\vec{\Omega}\cdot\vec{J}$ in the dual field theory with angular momentum $\vec{J}$.

$$D_M X = \partial_M X - iA_M X$$

AdS Boundary conditions

$$\chi|_{z=0} = m_q\zeta, \qquad A_\theta|_{z=0} = \Omega(r)r^2,$$

Inhomogeneous condensation

Y. Chen, Danning Li and M. Huang, Phys.Rev.D (2022)

Parameters $\left(m_q, v_3, v_4\right) = (0, -3{,}8)$, $\mu_0 = (0.43\ GeV)^2$, $\mu_1 = (0.83\ GeV)^2$, $\mu_2 = (0.176\ GeV)^2$

$$T_c \simeq 174 MeV$$

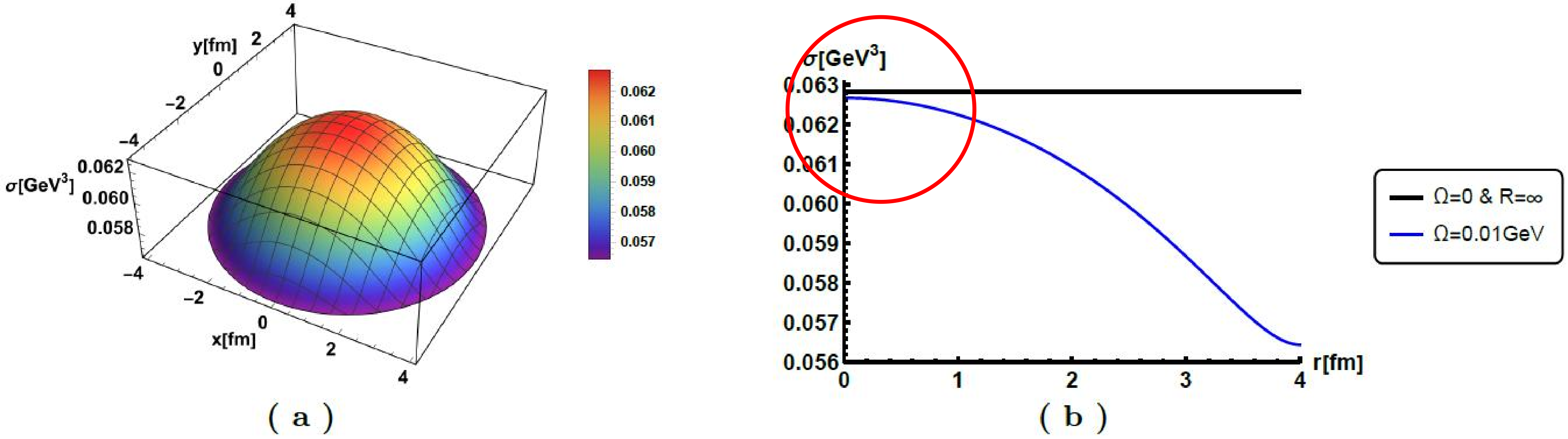

Figure 2. 3D and 2D plots of chiral condensation as a function of radial r at $T = 170$MeV and $\Omega = 0.01$ GeV with NBC and $(m_q, v_3, v_4) = (0, -3, 8)$. In Fig.(b), the black line indicates the value of condensation at the same temperature without rotation and finite size.

Tolman-Ehrenfest effect

Y. Chen, Danning Li and M. Huang, Phys.Rev.D (2022)

Different angular velocity distribution

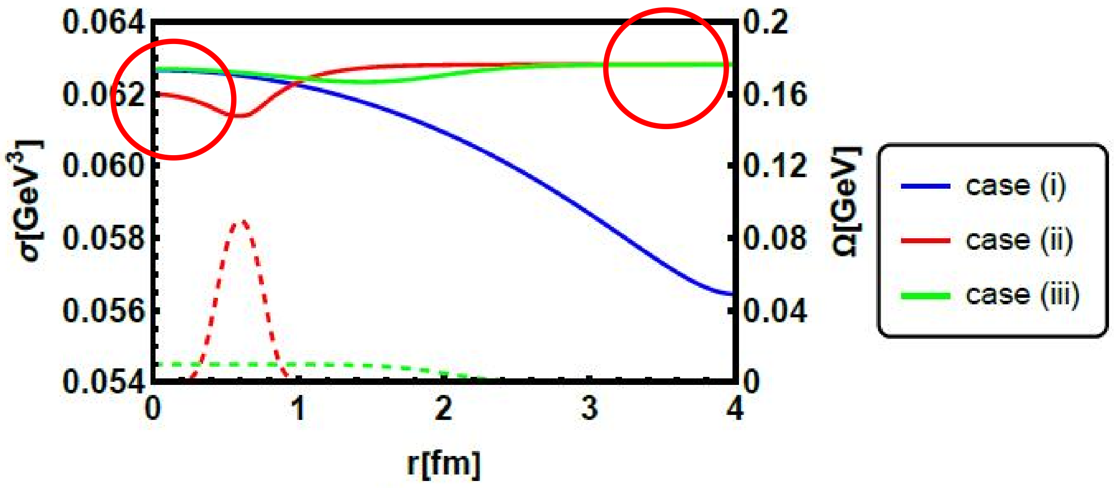

(a)

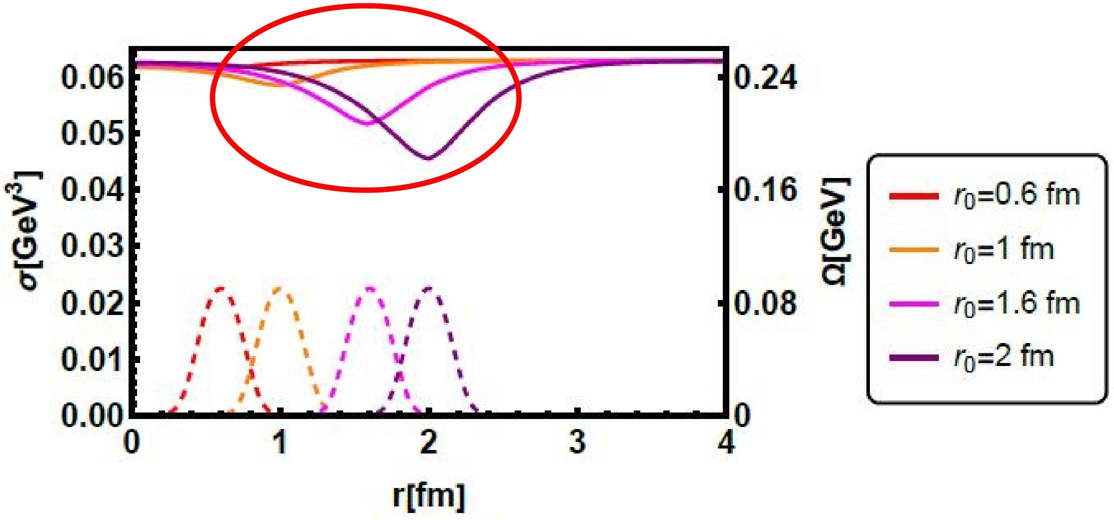

(b)

Figure 3. The chiral condensation as a function of radial r at $T = 170$ MeV with NBC and $(m_q, v_3, v_4) = (0, -3, 8)$, where the solid and dashed lines denote the profile of the condensation and the distribution of the angular velocity, respectively. In (a), the three cases of angular velocity distribution are: (i) $\Omega = 0.01$, (ii) $\Omega(r) = 0.18(\exp[1.5(r-10)^2]+1)^{-1}$ and (iii) $\Omega(r) = 0.01(\exp[(r-10)]+1)^{-1}$. Fig.(b) represents case (ii) $\Omega(r) = 0.18(\exp[1.5(r-r_0)^2]+1)^{-1}$ with $r_0 = 0.6$ fm, 1 fm, 1.6 fm and 2 fm.

$A_\theta \sim \Omega r^2$

$$\nu_4\chi^2 - \frac{A_\theta^2}{r^2})\chi = 0$$

$$\frac{\partial_r A_\theta}{} - \chi^2 A_\theta = 0$$

$$\frac{A_\theta^2}{r^2} \sim (\Omega r)^2 \sim (v)^2$$

Phase diagram

Y. Chen, Danning Li and M. Huang, Phys.Rev.D (2022)

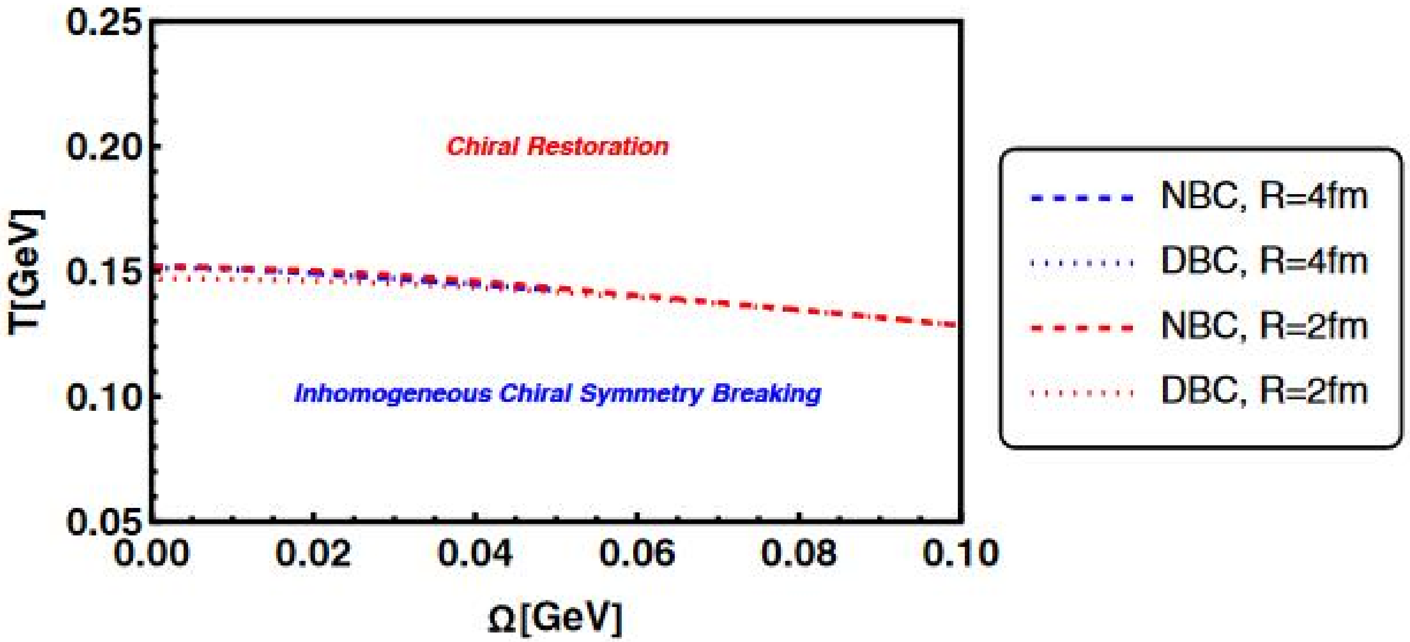

FIG. 13. The $T - \Omega$ phase diagram at fixed radius R is shown in the figure. Here, the red and blue lines correspond to radii of $R = 2$ and 4 fm, respectively, and the dashed and dotted lines represent NBC and DBC, respectively.

II. (a) Anisotropic background and deconfinement phase transition

DHQCD Model

Y. Chen, X. Chen, D. Li and M. Huang, arXiv:2405.06386

The dynamical holographic QCD (DHQCD) model with chemical potential is described by the Einstein-Maxwell-dilaton system. The action in the string frame can be written as

$$
\begin{aligned}
S^s_{\rm tot} &= S^s_G + S^s_M, \\
S^s_G &= \frac{1}{16\pi G_5}\int d^5x\sqrt{-g^s}e^{-2\Phi}\left[R^s + 4\partial_M\Phi\partial^M\Phi - V^s(\Phi) - \frac{h(\Phi)}{4}e^{\frac{4\Phi}{3}}F_{MN}F^{MN}\right], \\
S^s_M &= -\int d^5x\sqrt{-g^s}e^{-\Phi}\mathrm{Tr}\left[\nabla_M X^\dagger\nabla^M X + V_X(|X|, F_{MN}F^{MN})\right],
\end{aligned}
$$

potential reconstruction method

$$\Phi(z) = \mu_G^2 z^2 \tanh(\mu_{G^2}^4 z^2/\mu_G^2).$$

The DHQCD model can successfully describe hadron spectra, QCD phase transition, thermodynamical properties, transport properties of QCD matter.

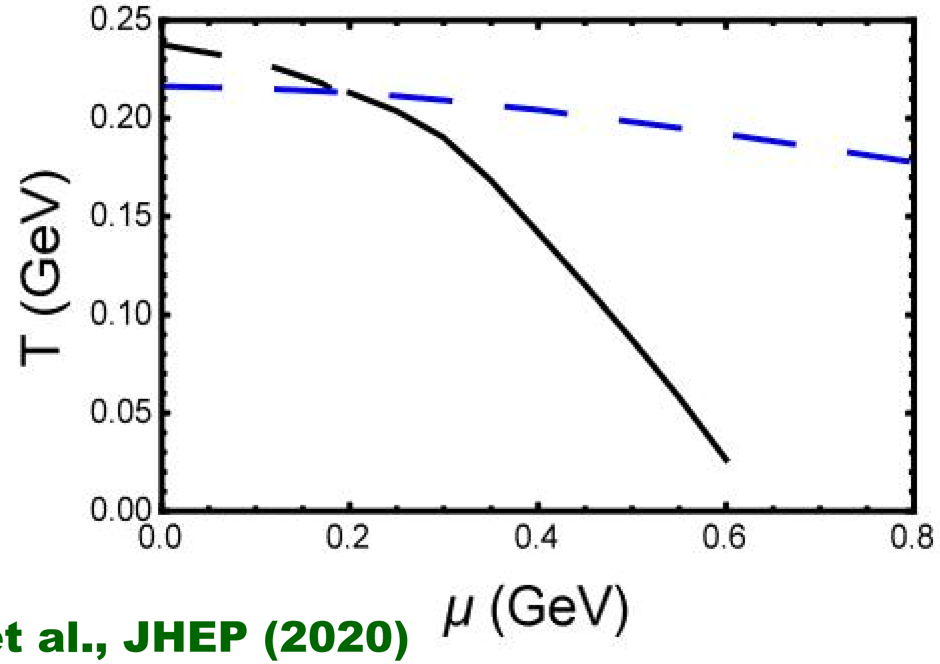

X. Chen, et al., JHEP (2020)

Model

Y. Chen, X. Chen, D. Li and M. Huang, arXiv:2405.06386

The action in the Einstein frame can be written as

$$S_G^e = \frac{1}{16\pi G_5}\int d^5x\sqrt{-g^e}\left[R^e - \frac{1}{2}\partial_M\Phi\partial^M\Phi - V^e(\Phi) - \frac{h(\Phi)}{4}F_{MN}F^{MN}\right],$$

The rotation is introduced by a non-zero polar angle component of the gauge field. It can be expanded as $A_\theta \sim \Omega r^2 + \rho_\theta$. Near the center, the current ρ_θ can be neglected and the gauge field is approximated as

$$A_M = (A_t, 0, 0, A_\theta, 0), \quad A_\theta = \Omega r^2,$$

And the background metric of the Einstein frame in the cylindrical coordinate system is

$$ds^2 = \frac{L^2 e^{2A_e(z)}}{z^2}[-f(z)dt^2 + \frac{dz^2}{f(z)} + e^{B(z)}dr^2 + r^2 e^{B(z)}d\theta^2 + e^{-2B(z)}dx_3^2],$$

Polarized dilaton

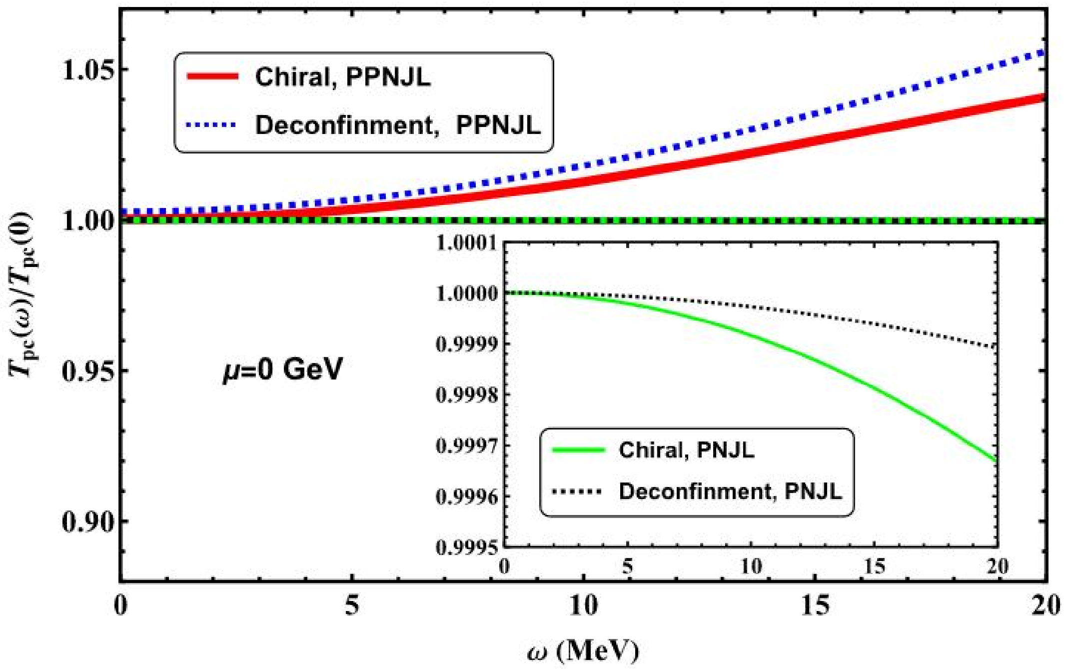

polarized Polyakov-loop potential in polarized-PNJL model

$$\frac{\mathcal{U}(\Phi,\bar{\Phi},T,\omega)}{T^4} = -Cf(T,\omega)\left(\frac{T}{T_0}\right)^2\Phi\bar{\Phi} - \frac{1}{3}(\Phi^3+\bar{\Phi}^3) + C^{-1}f^{-1}(T,\omega)\left(\frac{T}{T_0}\right)^{-2}\Phi^2\bar{\Phi}^2,$$

F. Sun, et al., Phys.Rev.D (2024)

We considering the polarization of the gluo-dynamics induced by the rotation

$$\Phi(z,\Omega) = \mu_G(\Omega)^2 z^2 \tanh(\mu_{G^2}(\Omega)^4 z^2/\mu_G(\Omega)^2).$$

$\mu_G(\Omega)$ can be expanded as

$$\mu_G + \mu_\Omega\Omega^2 + \mu_{\Omega_2}\Omega^4 + \ldots$$

$$\Phi = (\mu_G + \mu_\Omega\Omega^2)^2 z^2 \tanh(\mu_{G^2}^4 z^2/(\mu_G + \mu_\Omega\Omega^2)^2).$$

Y. Chen, et al., arXiv:2405.06386

Results

Y. Chen, X. Chen, D. Li and M. Huang, arXiv:2405.06386

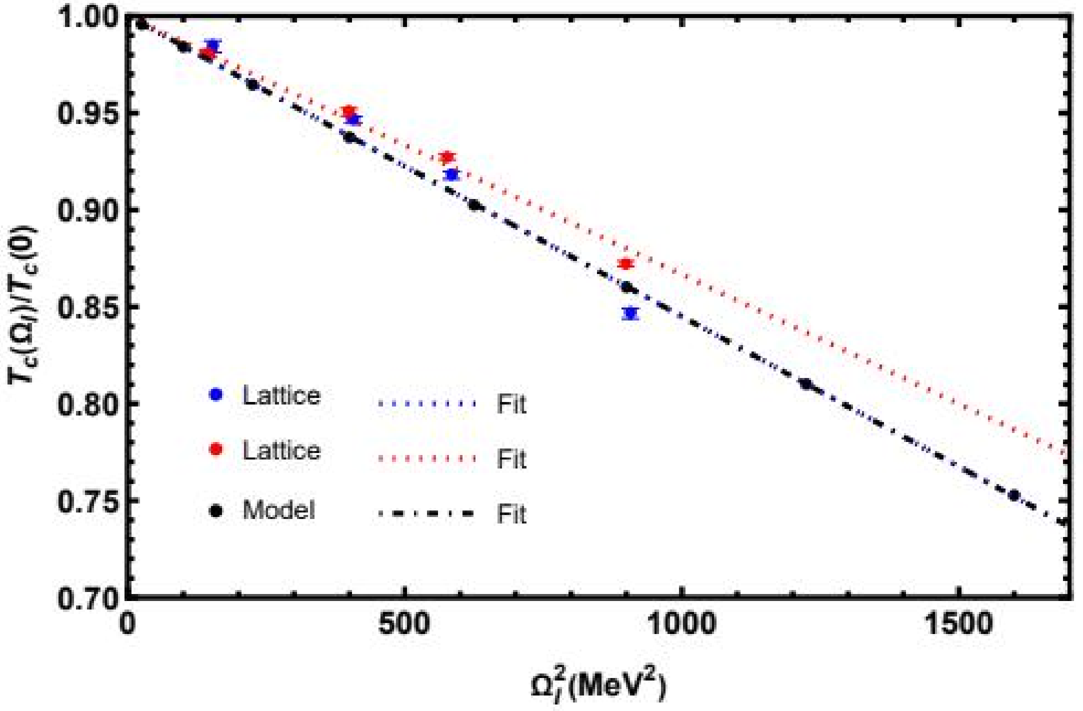

The only parameter μ_Ω to be determined in the DHQCD model is based on the relationship between the phase transition temperature $T_c(\Omega_I)$ and the imaginary angular velocity predicted by lattice QCD.

$$T_c(\Omega_I)/T_c(0) = 1 - C_2\Omega_I^2$$

Results

Y. Chen, X. Chen, D. Li and M. Huang, arXiv:2405.06386

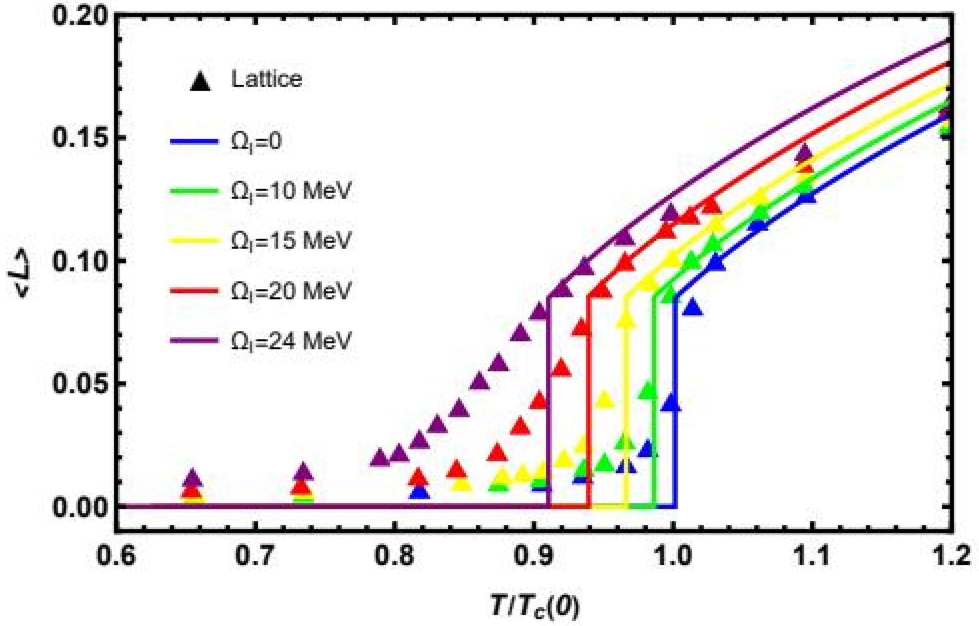

(a) imaginary rotation

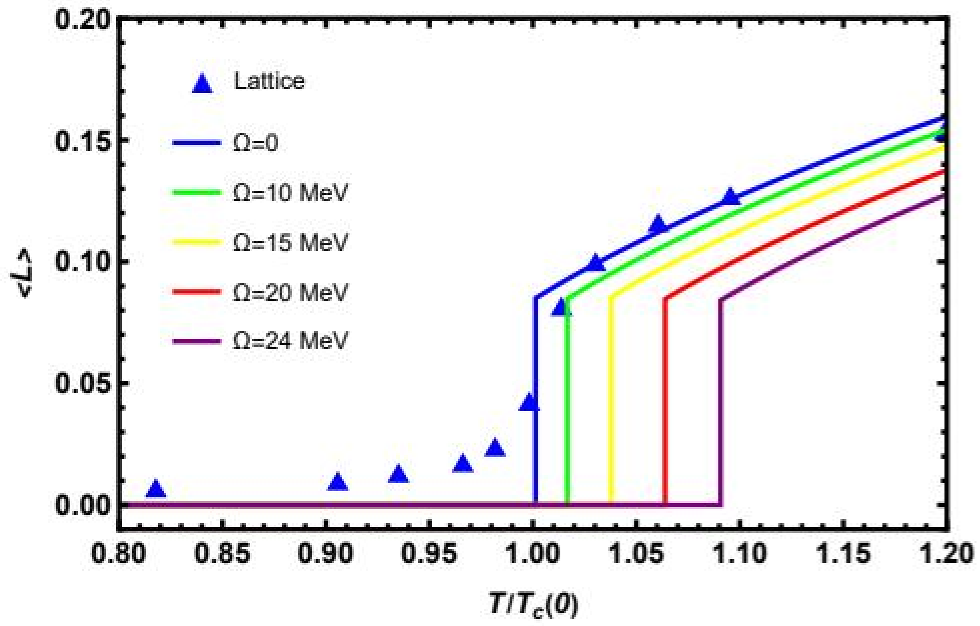

(b) real rotation

FIG. 4. The expectation value of the Polyakov loop $\langle L \rangle$ obtained from the DHQCD model for pure gluon system and lattice as a function of temperature under both real and imaginary rotation. The triangles in the figure represent the lattice QCD data [100] and the solid lines are the model calculations.

Results

Y. Chen, X. Chen, D. Li and M. Huang, arXiv:2405.06386

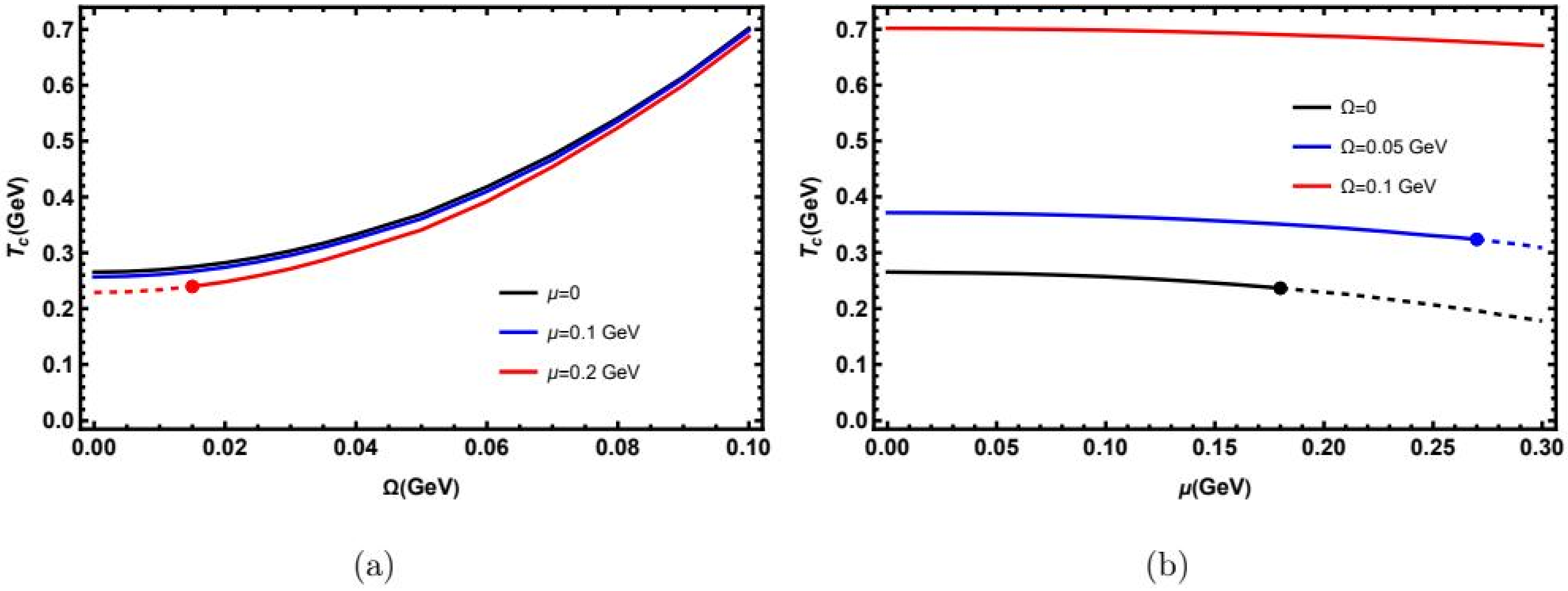

FIG. 5. The $T-\Omega$ and $T-\mu$ phase diagrams of deconfinement phase transition for the pure gluon system.

Results

Y. Chen, X. Chen, D. Li and M. Huang, arXiv:2405.06386

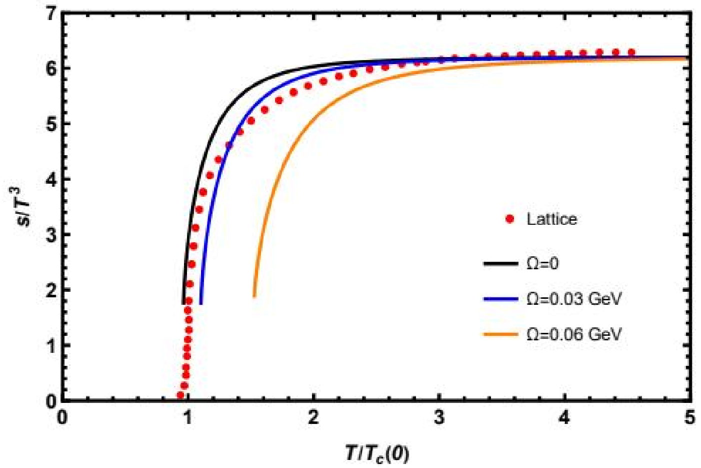

(a) entropy density

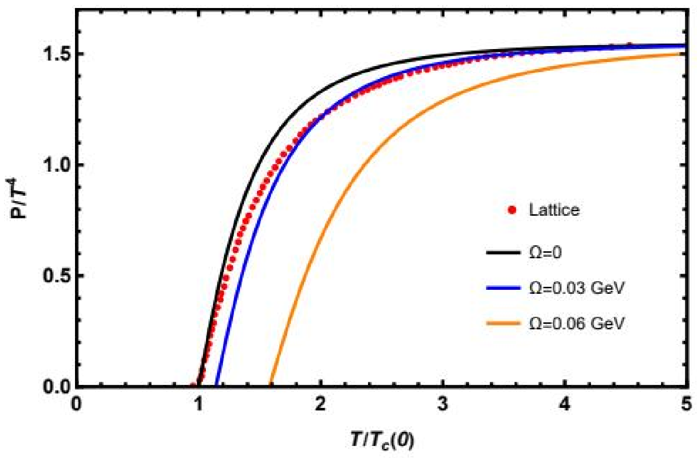

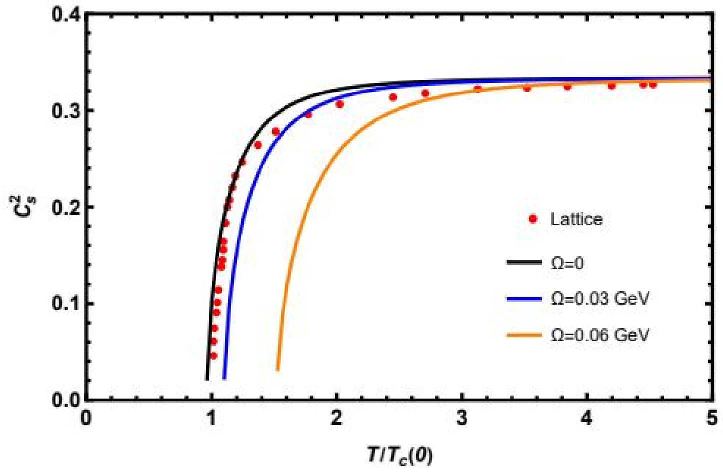

nd velocity

$$Q_{uantites}(T,\ \Omega) \simeq Q(T(1+C_2\Omega^2),0)$$

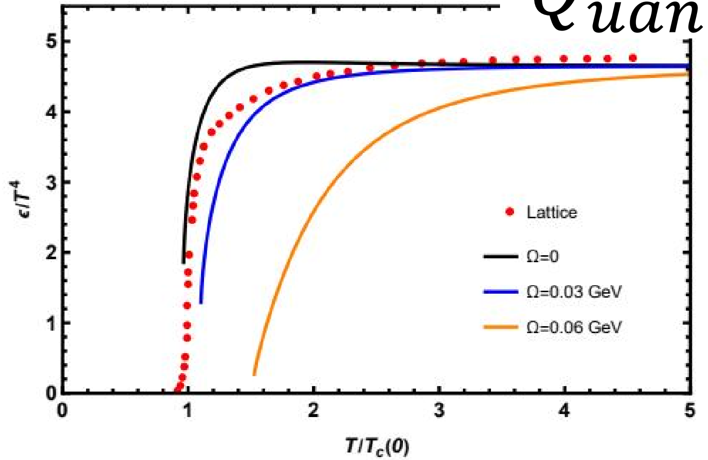

(c) energy density

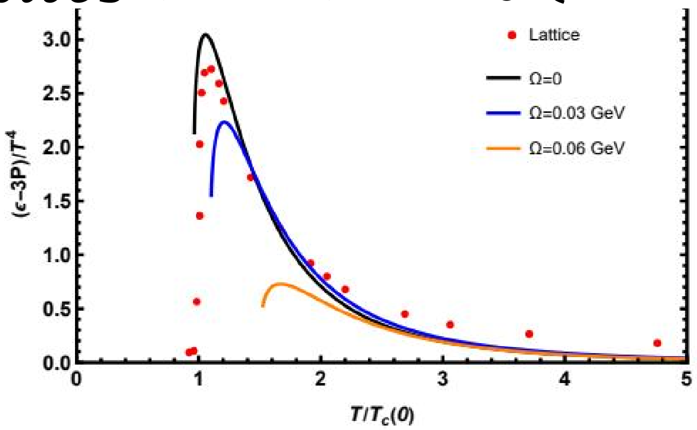

(d) trace anomaly

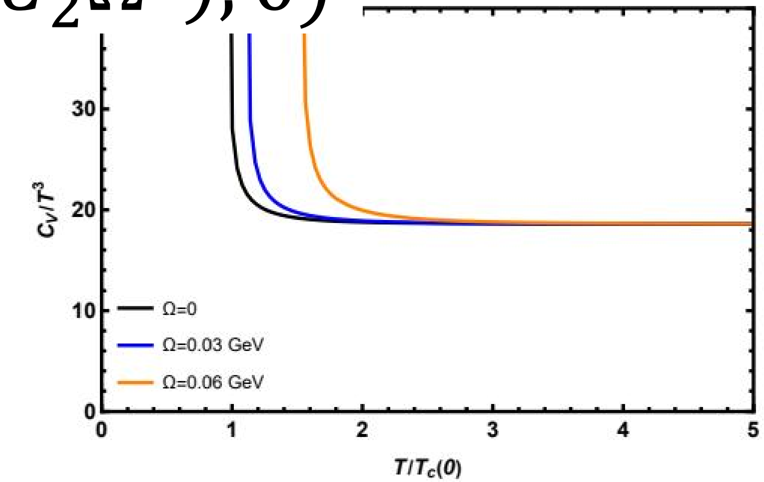

(b) specific heat

II. (b) Chiral phase transition under rotation

DHQCD Model

Y. Chen, X. Chen, D. Li and M. Huang, arXiv:2405.06386

The DHQCD model can be written as

$$D_M X = \partial_M X - iA_M X$$

$$\begin{aligned} S^s_{\rm tot} &= S^s_G + S^s_M, \\ S^s_G &= \frac{1}{16\pi G_5}\int d^5x\sqrt{-g^s}e^{-2\Phi}\left[R^s + 4\partial_M\Phi\partial^M\Phi - V^s(\Phi) - \frac{h(\Phi)}{4}e^{\frac{4\Phi}{3}}F_{MN}F^{MN}\right], \\ S^s_M &= -\int d^5x\sqrt{-g^s}e^{-\Phi}{\rm Tr}\left[\nabla_M X^\dagger\nabla^M X + V_X(|X|, F_{MN}F^{MN})\right], \end{aligned}$$

The potential of action is considered as the following form

$$V_X(|X|, F_{MN}F^{MN}) = \left(\frac{m_5^2}{2} + \lambda_2 F^2\right)\chi^2 + (v_4 + \lambda_4 F^2)\chi^4 + (v_6 + \lambda_6 F^2)\chi^6,$$

√

The equation of motion of scalar field can be obtained as

$$- \frac{8e^{-2(A_s+B)}}{f}\chi\Omega^2 z^2\left(\lambda_2 + \lambda_4\chi^2 + \lambda_6\chi^4\right) + \frac{2e^{-2A_s}}{f}\chi A_t'^2 z^2\left(\lambda_2 + \lambda_4\chi^2 + \lambda_6\chi^4\right)$$
$$- \frac{e^{2A_s}}{fz^2}\chi\left(-3 + 4v_4\chi^2 + 6v_6\chi^4\right) + \left(3A_s' + \frac{f'}{f} - \Phi' - \frac{3}{z}\right)\chi' + \chi'' = 0,$$

Results

Y. Chen, X. Chen, D. Li and M. Huang, arXiv:2405.06386

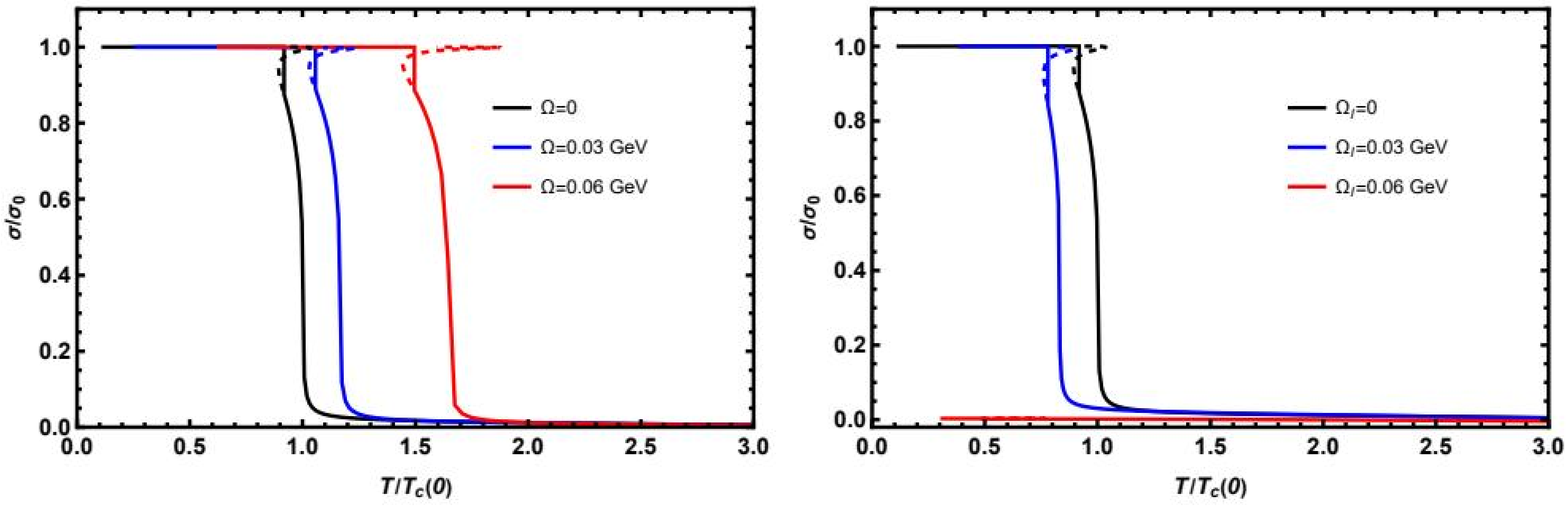

(a) real rotation

(b) imaginary rotation

FIG. 6. The chiral condensate for 2-flavor system as a function of temperature at different angular velocities and imaginary angular velocities with chemical potential $\mu = 0.12$ GeV. In the figure σ_0 is the maximum value of condensation and $T_c(0)$ is the critical temperature with zero angular velocity.

Results

Y. Chen, X. Chen, D. Li and M. Huang, arXiv:2405.06386

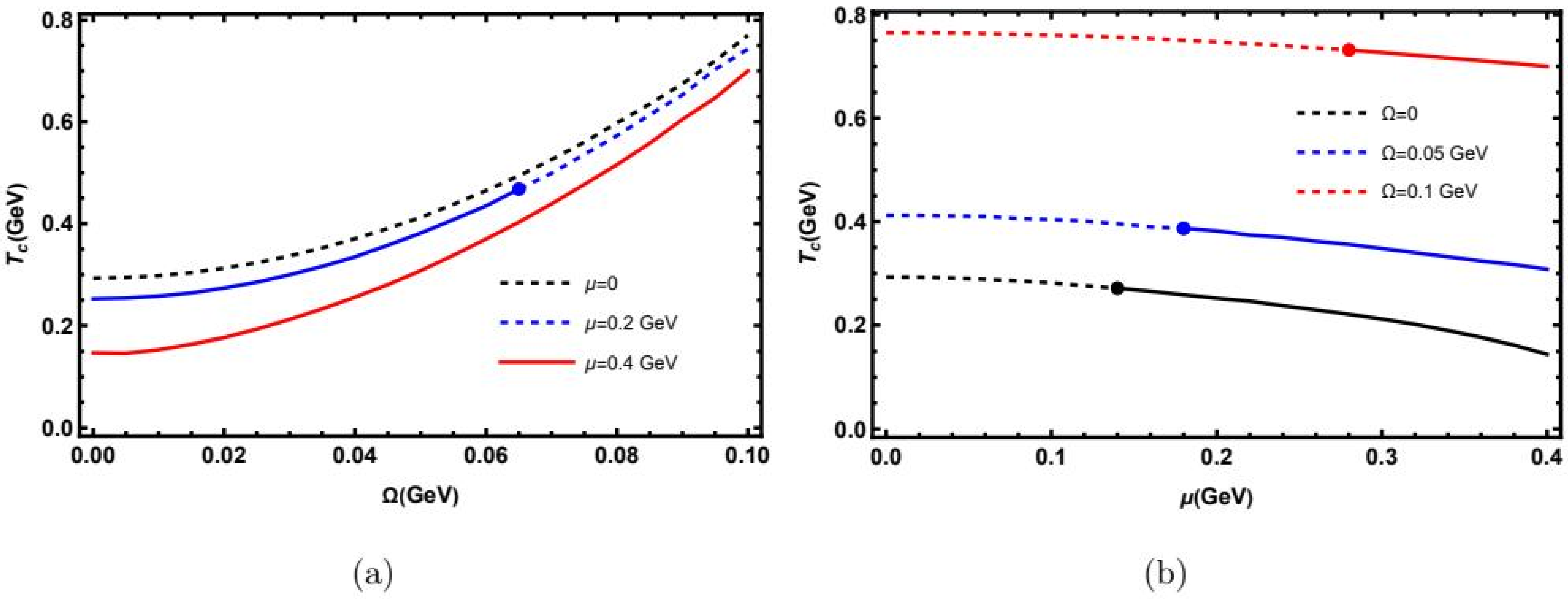

FIG. 7. The $T-\Omega$ and $T-\mu$ phase diagrams of chiral phase transition for 2-flavor system.

III. Pion Condensation

Phase Diagram

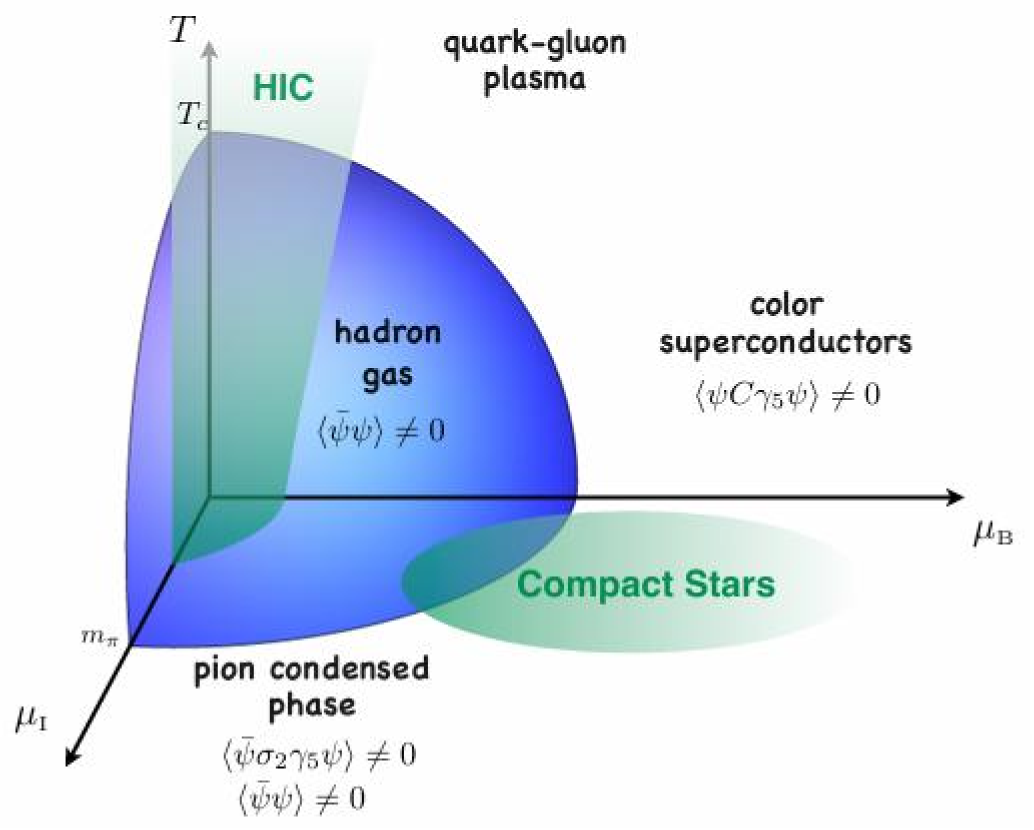

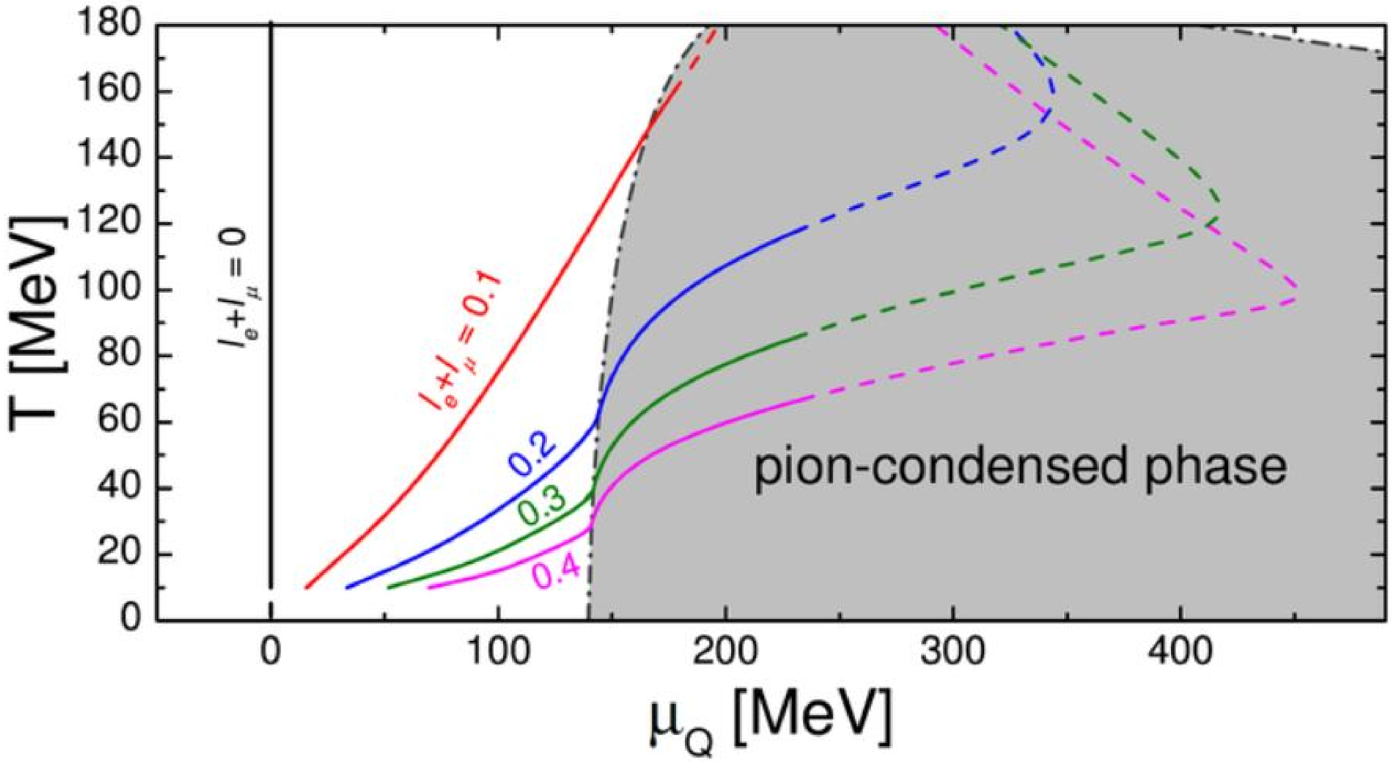

Vovchenko et al., PRL126, 012701 (2021)

Mannarelli, Particles (2019)

Model

Y. Chen, M. Ding, K. Bitaghsir Fadafan,
D. Li and M. Huang, arXiv: 2408.17080

The holographic QCD model with Nf = 2 is constructed from SU(2)L × SU(2)R ≡ SU(2)V × SU(2)A flavor symmetry. The probe action is given as

$$S_{KKSS} = -\int d^4x \int_0^{z_h} dz\sqrt{-g}e^{-\Phi}Tr\left[|DX|^2 + m_5^2(z)|X|^2 + \lambda|X|^4 + \frac{1}{4g_5^2}(F_V^2 + F_A^2)\right]$$

The vacuum of scalar corresponds to sigma condensate and pion condensate can be given as $X = \frac{1}{2}(\Sigma t^0 + \Pi^a t^a)$. The nonzero gauge field of model is $V_0^{(3)} = \mu_I - \rho_I z^2$, with isospin chemical potential and isospin density. And the background metric is AdS-black hole

$$ds^2 = \frac{L^2}{z^2}\left[-f(z)dt^2 + d\vec{x}^2 + \frac{dz^2}{f(z)}\right]$$

we have considered two possible forms of the five-dimensional mass squared as follows:

$$m_5^2(z) = -3 - \mu_c^2 z^2, \qquad \text{(SW-I)}$$

$$m_5^2(z) = -3\left(1 + \gamma_m \tanh\left[\kappa\Phi(z)\right]\right), \qquad \text{(SW-II)}$$

Model

Y. Chen, M. Ding, K. Bitaghsir Fadafan, D. Li and M. Huang, arXiv: 2408.17080

The equations of motion of the holographic model are obtained as

$$\frac{\lambda\Sigma^3}{2z^2}+\frac{v\Pi a_2}{f}+\left(-\frac{a_2^2}{f}+\frac{\lambda\Pi^2+2m_5^2(z)}{2z^2}\right)\Sigma+\left(-f'+f\left(\frac{3}{z}+\Phi'\right)\right)\Sigma'-f\Sigma''=0, \quad (22)$$

$$\frac{\lambda\Pi^3}{2z^2}+\frac{v\Sigma a_2}{f}+\left(-\frac{v^2}{f}+\frac{\lambda\Sigma^2+2m_5^2(z)}{2z^2}\right)\Pi+\left(-f'+f\left(\frac{3}{z}+\Phi'\right)\right)\Pi'-f\Pi''=0, \quad (23)$$

$$\frac{g_5^2\Sigma}{z^2}(v\Pi-a_2\Sigma)+\left(-\frac{f}{z}-f\Phi'\right)a_2'+fa_2''=0, \quad (24)$$

$$\frac{g_5^2\Pi}{z^2}(a_2\Sigma-v\Pi)+\left(-\frac{f}{z}-f\Phi'\right)v'+fv''=0. \quad (25)$$

For the (pseudo-)scalar fields, the expansions are

$$\Sigma\to m_q\zeta z+\frac{\langle\sigma\rangle}{\zeta}z^3+\mathcal{O}(z^3), \qquad \Pi^a\to\frac{\langle\pi^a\rangle}{\zeta}z^3+\mathcal{O}(z^3),$$

Condensation

Y. Chen, M. Ding, K. Bitaghsir Fadafan,
D. Li and M. Huang, arXiv: 2408.17080

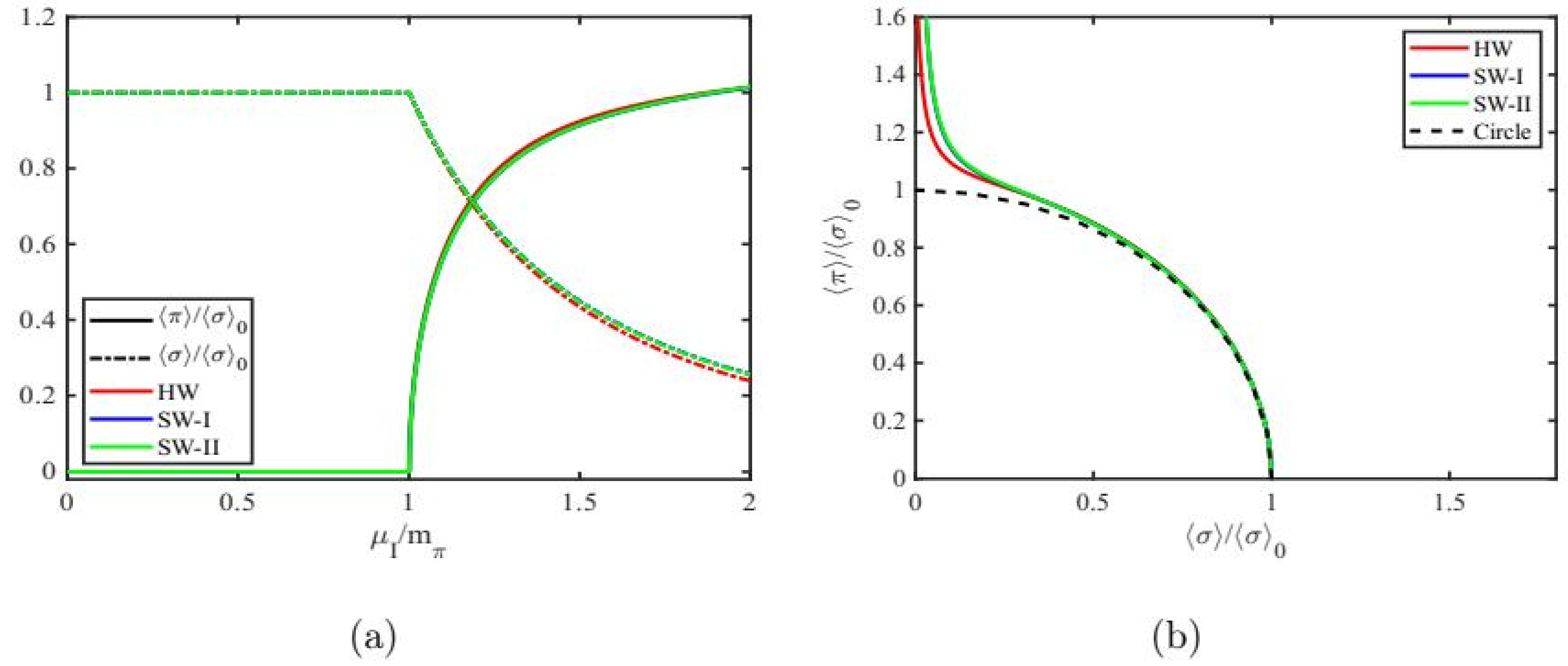

FIG. 1. Panel (a) illustrates how the sigma and pion condensates vary with the isospin chemical potential μ_I in both the HW and SW models. Panel (b) reveals the interrelationship between the sigma and pion condensates, where the black dashed line represents the unit circle.

Condensation

Y. Chen, M. Ding, K. Bitaghsir Fadafan,
D. Li and M. Huang, arXiv: 2408.17080

According to χPT, the expressions for isospin density and axial-vector condensation can be simplified to

$$n_I = f_\pi^2 \mu_I \left(1 - \frac{m_\pi^4}{\mu_I^4}\right) \Theta(\mu_I - m_\pi), \qquad \langle\sigma\rangle_A = \frac{f_\pi^2 m_\pi^2}{\mu_I} \sqrt{1 - \frac{m_\pi^4}{\mu_I^4}} \Theta(\mu_I - m_\pi),$$

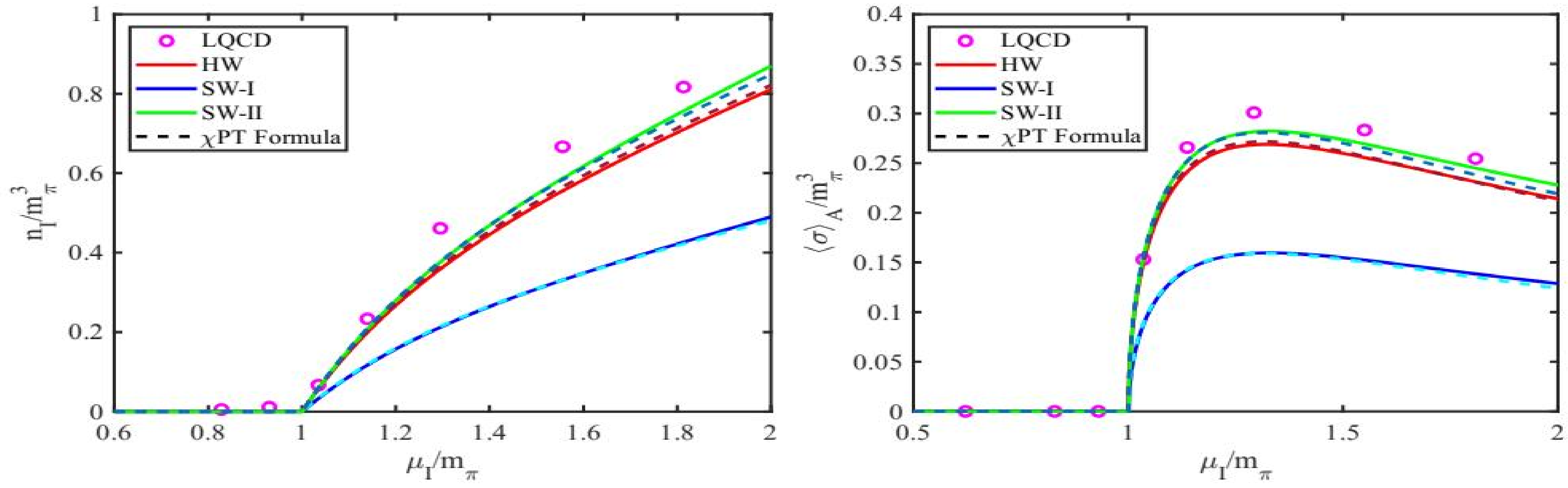

FIG. 2. The isospin density and axial vector condensate as a function of isospin chemical potential μ_I in HW and SW model. The black dashed lines are calculations from χPT formulas (29) and (30).

Thermodynamics

Y. Chen, M. Ding, K. Bitaghsir Fadafan,
D. Li and M. Huang, arXiv: 2408.17080

At zero temperature, the pionic pressure p and energy density ϵ can be given by thermodynamic relations

$$p = \frac{\log \mathcal{Z}_{\mathrm{QCD}}}{V} = \int_0^{\mu_I} d\mu_I' n_I(\mu_I'), \qquad \epsilon = -p + \mu_I n_I.$$

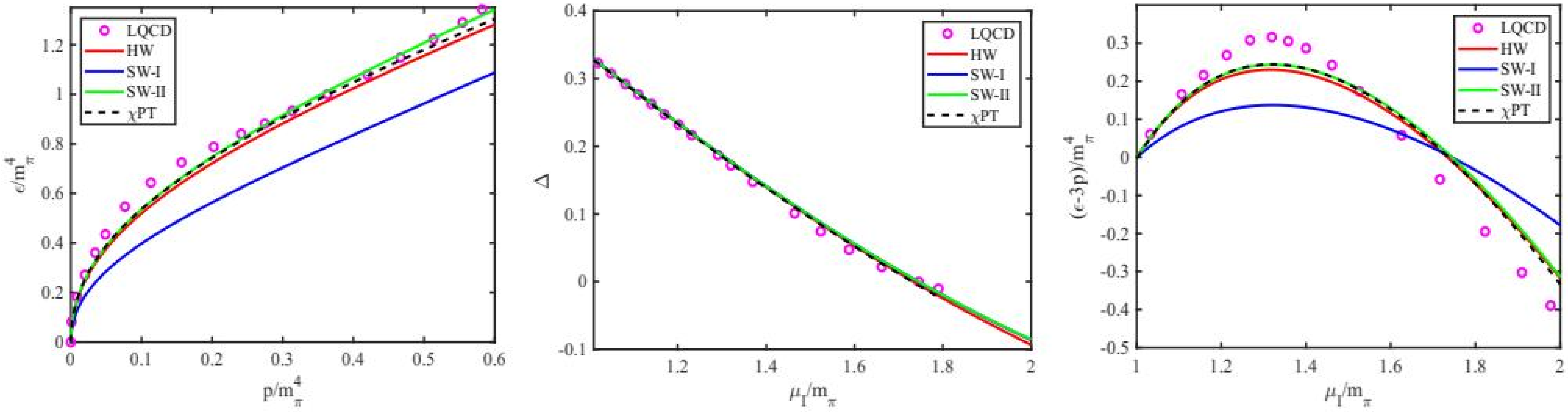

(a) (b) (c)

FIG. 3. The equation of state, normalized trace anomalies $\Delta = 1/3 - p/\epsilon$ and $(\epsilon - 3p)/m_\pi^4$ in HW and SW model. The magenta circles represent lattice QCD data [7]. The black dashed lines are calculations from χPT [22].

Thermodynamics

Y. Chen, M. Ding, K. Bitaghsir Fadafan,
D. Li and M. Huang, arXiv: 2408.17080

The square of the speed of sound and adiabatic index is given as are defined as

$$c_s^2 = \frac{\partial p}{\partial \epsilon}, \qquad \gamma = \frac{d\log p}{d\log \epsilon} = \frac{\epsilon}{p} c_s^2.$$

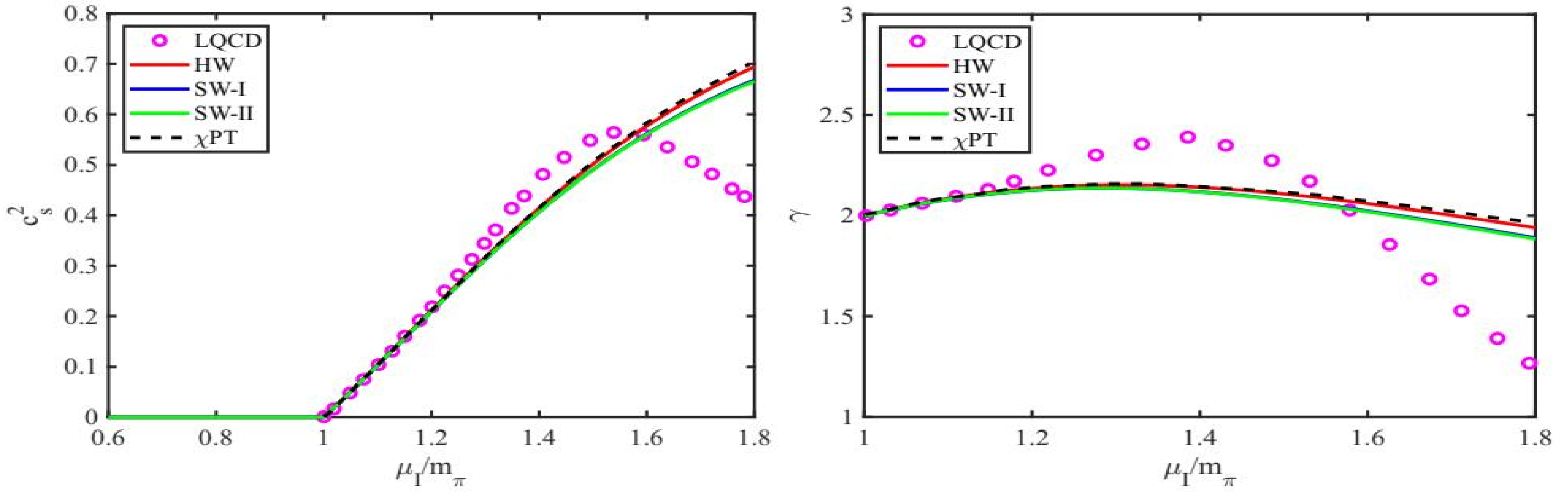

FIG. 4. The speed of sound and the adiabatic index as a function of the isospin chemical potential in the HW and SW models. The black dashed lines are calculations from χPT and the magenta circles are the lattice QCD data from Ref. [22].

Pion Star

Y. Chen, M. Ding, K. Bitaghsir Fadafan,
D. Li and M. Huang, arXiv: 2408.17080

The form of the TOV equations are as follow

$$\frac{d}{dr}p(r) + [p(r)+\epsilon(r)]\frac{G\left[m(r)+4\pi r^3 P(r)\right]}{r^2\left[1-2\frac{Gm(r)}{r}\right]} = 0,$$

$$\frac{d}{dr}m(r) - 4\pi r^2\epsilon(r) = 0,$$

The dimensionless tidal deformability Λ

$$\Lambda = \frac{2k_2}{3C^5},$$

where

$$k_2 = \frac{8C^5}{5}(1-2C)^2[2+2C(y-1)-y]\left\{2C[6-3y+3C(5y-8)]\right.$$
$$+\,4C^3\left[13-11y+C(3y-2)+2C^2(1+y)\right]$$
$$\left.+\,3(1-2C)^2[2-y+2C(y-1)]\ln(1-2C)\right\}^{-1},$$

Pion Star

Y. Chen, M. Ding, K. Bitaghsir Fadafan,
D. Li and M. Huang, arXiv: 2408.17080

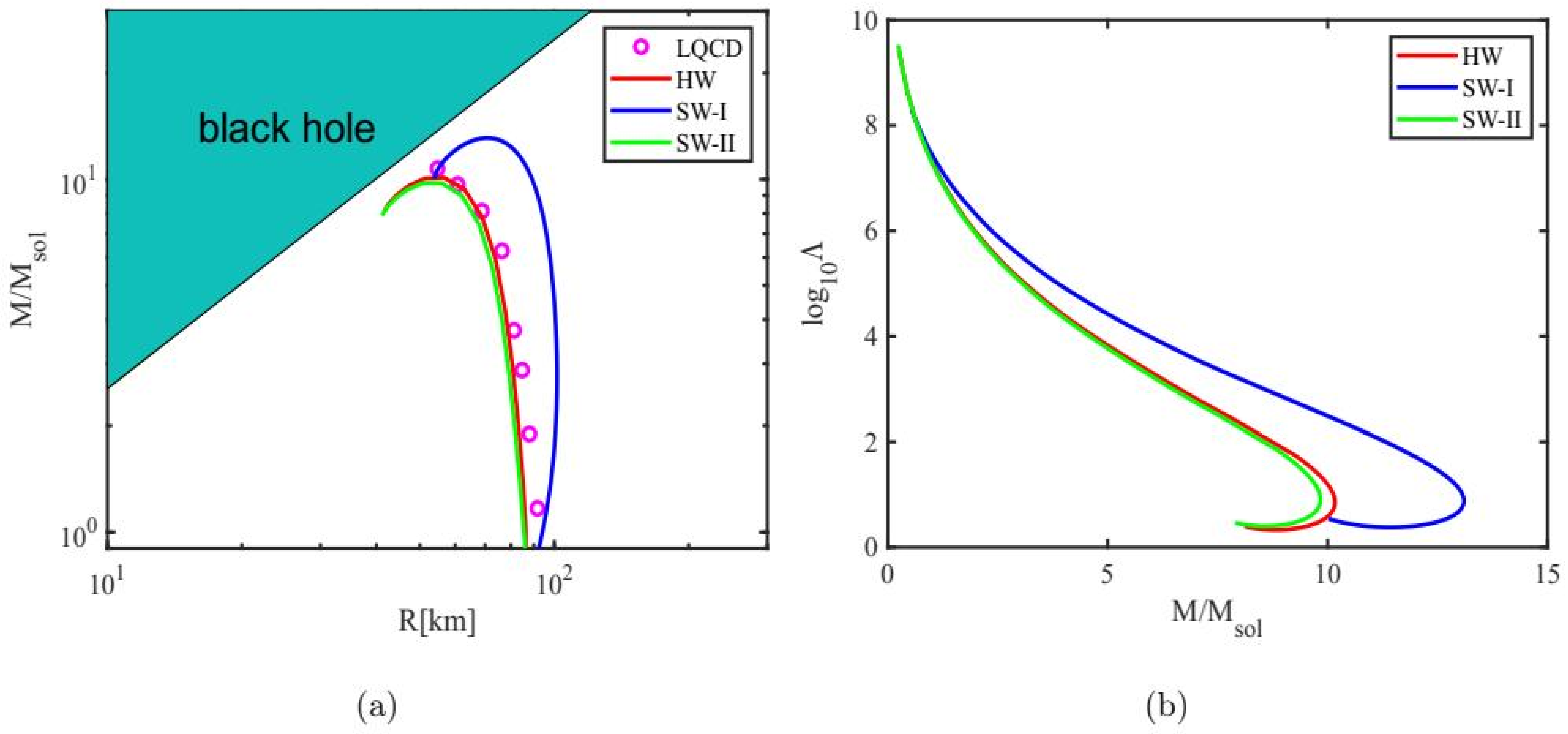

FIG. 5. The mass-radius relation and tidal deformability of pion stars. The magenta circles are the mass-radius relation obtained through the equation of state from lattice QCD data Ref. [22].

IV. Conclusion and discussion

Summary

1) We use a new approach to investigate the effect of rotation on deconfinement and chiral phase transitions in the dynamical holographic QCD model. Our holographic calculations are consistent with lattice QCD data.

① the non-trivial term $A_\theta = \Omega r^2$ in the gauge field

② polarization of the gluo-dynamics induced by the rotation (the Ω dependent dilaton field)

Summary

2) In the DHQCD model, the effect of rotation on the deconfinement phase transition and the chiral restoration phase transition shows consistency. Both the critical temperatures decrease/increase with imaginary/real angular velocity as $\frac{T}{T_c} \sim 1 - C_2\Omega_I^2$ and $\frac{T}{T_c} \sim 1 + C_2\Omega^2$, which is consistent with lattice QCD results.

3) We found that the effect of rotation on the entropy density, pressure, square of the speed of sound, and specific heat can be approximated by the relationship $Q(T,\Omega) \simeq Q)T(1 + C_2\Omega^2), 0($

Summary

4) The results from the holographic models show good agreement with lattice QCD in terms of isospin density, axial-vector condensation, EoS, and normalized trace anomaly. However, discrepancies were found in the calculations of the sound speed and adiabatic index.

5) Further analysis shows that the results from the holographic models are very similar to those from χPT.

Thanks !